Standard Model of Particle Physics

Lecture Course at Heidelberg University
Summer term 2024

5. Quantum Chromodynamics

Carlo Ewerz
Institut für Theoretische Physik

Skyler Degenkolb, Ulrich Uwer
Physikalisches Institut

Heidelberg University

Colour SU(3)

- Hadronic matter is made of quarks of different flavours. Approximate $\mathrm{SU}(3)_f$ flavour symmetry is observed in spectrum of lowest-lying mesons and baryons.

- The known quarks and their properties are

Quark	Charge	Mass	Isospin
u	$+2/3$	$\sim$ 4 MeV	$+1/2$
d	$-1/3$	$\sim$ 7 MeV	$-1/2$
c	$+2/3$	$\sim$ 1.5 GeV	0
s	$-1/3$	$\sim$ 135 MeV	0
t	$+2/3$	$\sim$ 173 GeV	0
b	$-1/3$	$\sim$ 5 GeV	0

- Additional quantum number colour with three possible values was introduced for quarks in order to cure problem with statistics of spin-$\frac{3}{2}$ baryons.

- Only colour singlet states exist in nature. If group of transformations colour is SU(3), the basic colour singlet states are mesons $\bar{q}_f q_{f'}$ and baryons $\varepsilon_{abc} q_a q_b q_c$.

- There now is sound proof of validity of colour SU(3).

  ⋆ Early evidence for the number of colours $N_c = 3$ came from rate of decay $\pi^0 \to \gamma\gamma$.

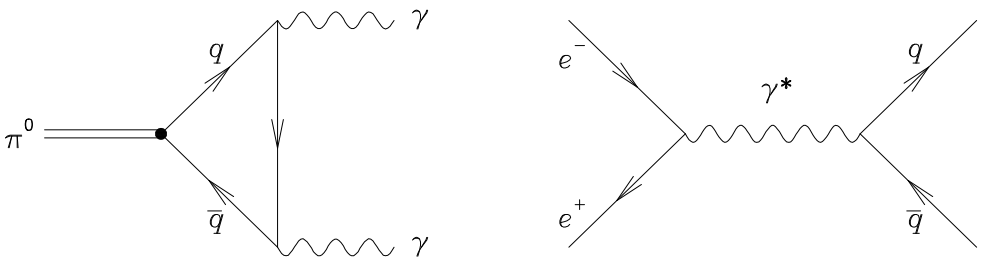

(a) (b)

  ⋆ Another test of number of colours of charged fundamental constituents is ratio R of e^+e^- total hadronic cross section to cross section for muon pairs, diagram (b). (See also later). At low energy virtual photon excites only u, d, s quarks, each of which occurs in 3 colours. Therefore

$$R = 3\left[\left(\frac{2}{3}\right)^2 + \left(-\frac{1}{3}\right)^2 + \left(-\frac{1}{3}\right)^2\right] = 2$$

For center-of-mass energies $E_{\rm cm} \geq 10\,\text{GeV}$ one is above threshold for production of c, b quarks, and hence

$$R = 3\left[2 \times \left(\frac{2}{3}\right)^2 + 3 \times \left(-\frac{1}{3}\right)^2\right] = \frac{11}{3}$$

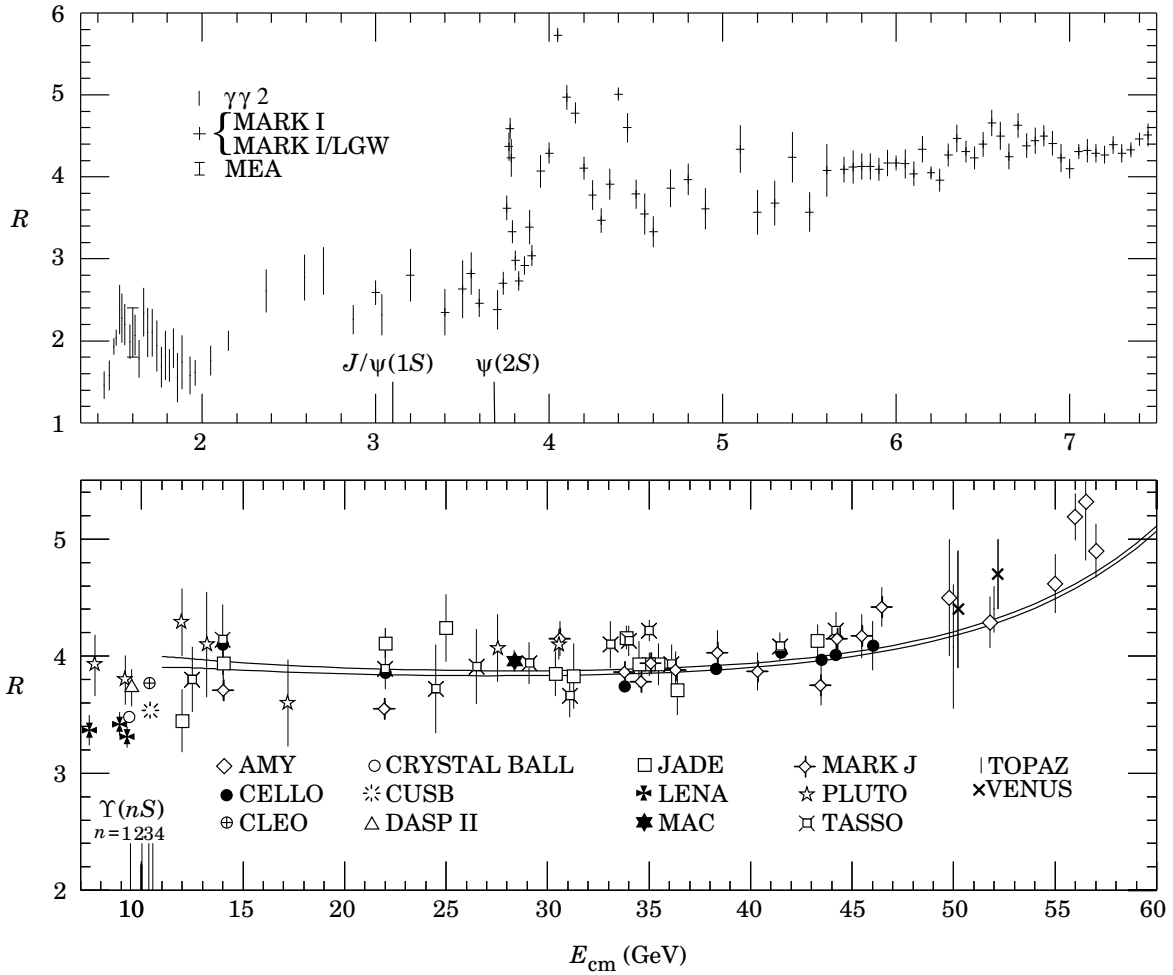

- Existence of approximately point-like constituents inside hadrons was known from electron deep inelastic scattering experiments at SLAC. Measured cross section did not fall exponentially with inelasticity but showed approximate scaling behaviour, indicative of point-like structure inside target nucleons.
  This gave rise to parton model. Partons are now known to be coloured quarks and gluons.

- Discovery of asymptotic freedom of QCD gave an answer to question why quarks behave as almost free particles when probed at small distances: coupling between quarks and gluon decreases with decreasing distance.

Quantum Chromodynamics

* Strong interactions are described by **Quantum Chromodynamics (QCD)**:
Quarks come in 3 "colours" ($a = 1, 2, 3$) and the gauge transformations are represented by $SU(3)$ matrices,

$$q_a(x) \longrightarrow q'_a(x) = U_{ab}(x)\, q_b(x)$$

$$U_{ab}(x) = e^{i \underline{t} \cdot \underline{\theta}(x)}$$

$$\underline{t} \cdot \underline{\theta} \equiv \sum_{A=1}^{8} t^A \theta^A$$

The generators $t^A = \frac{1}{2}\lambda_A$ are given in terms of Gell-Mann matrices λ_A:

$$\lambda_1 = \begin{pmatrix} 0 & 1 & 0 \\ 1 & 0 & 0 \\ 0 & 0 & 0 \end{pmatrix} \quad \lambda_2 = \begin{pmatrix} 0 & -i & 0 \\ i & 0 & 0 \\ 0 & 0 & 0 \end{pmatrix} \quad \lambda_3 = \begin{pmatrix} 1 & 0 & 0 \\ 0 & -1 & 0 \\ 0 & 0 & 0 \end{pmatrix}$$

$$\lambda_4 = \begin{pmatrix} 0 & 0 & 1 \\ 0 & 0 & 0 \\ 1 & 0 & 0 \end{pmatrix} \quad \lambda_5 = \begin{pmatrix} 0 & 0 & -i \\ 0 & 0 & 0 \\ i & 0 & 0 \end{pmatrix} \quad \lambda_6 = \begin{pmatrix} 0 & 0 & 0 \\ 0 & 0 & 1 \\ 0 & 1 & 0 \end{pmatrix}$$

$$\lambda_7 = \begin{pmatrix} 0 & 0 & 0 \\ 0 & 0 & -i \\ 0 & i & 0 \end{pmatrix} \quad \lambda_8 = \frac{1}{\sqrt{3}} \begin{pmatrix} 1 & 0 & 0 \\ 0 & 1 & 0 \\ 0 & 0 & -2 \end{pmatrix}$$

Note that λ_3 and λ_8 are diagonal.

* $$\underline{t} \cdot \underline{t} = C_F \cdot \mathbb{1}$$

$C_F = \frac{4}{3}$ – "quark colour charge squared"

* $[t^A, t^B] = i f^{ABC} t^C$

with the structure constants f^{ABC} of $SU(3)$.

f^{ABC} are antisymmetric and

$$f^{123} = 1$$

$$f^{147} = -f^{156} = f^{246} = f^{257} = f^{345} = -f^{367} = \frac{1}{2}$$

$$f^{458} = f^{678} = \frac{\sqrt{3}}{2}$$

* $\sum_{A,B} f^{ABC} f^{ABD} = C_A \delta_{CD}$

$C_A = 3$ – "gluon colour charge squared"

* The QCD Lagrangian density is

$$\mathcal{L}_{QCD} = -\frac{1}{4} F^A_{\mu\nu} F^{A\mu\nu} + \sum_{\substack{\text{flavours} \\ f}} \bar{q}^f_a \left(i \not{D}_{ab} - m_q \delta_{ab} \right) q^f_b$$

with

$$F^A_{\mu\nu} = \partial_\mu A^A_\nu - \partial_\nu A^A_\mu - g_s f^{ABC} A^B_\mu A^C_\nu$$

and the covariant derivative

$$(D_\mu)_{ab} = \partial_\mu \delta_{ab} + i g_s \left(\underline{t} \cdot \underline{A}_\mu \right)_{ab}$$

A^A_μ are the gluon fields ($A = 1, \ldots, 8$)

and g_s is the (bare) QCD coupling with

$$\alpha_s \equiv \frac{g_s^2}{4\pi} .$$

* For gauge invariance of $\mathcal{L}_{QCD}$ we need

$$D_\mu q \to D'_\mu q' = U D_\mu q \,.$$

Now

$$D'_\mu q' = (\partial_\mu + ig \underline{t}\cdot \underline{A}'_\mu) U q$$
$$= (\partial_\mu U) q + U \partial_\mu q + ig \underline{t}\cdot \underline{A}'_\mu U q$$

and

$$U D_\mu q = U \partial_\mu q + ig U \underline{t}\cdot \underline{A}_\mu q$$

Hence we need

$$ig \underline{t}\cdot \underline{A}'_\mu U = ig U \underline{t}\cdot \underline{A}_\mu - (\partial_\mu U)$$

$$\Rightarrow \quad \underline{t}\cdot \underline{A}'_\mu = U \underline{t}\cdot \underline{A}_\mu U^+ + \frac{i}{g}(\partial_\mu U) U^+$$

* The field strength tensor $F^A_{\mu\nu}$ then transforms according to

$$\underline{t}\cdot \underline{F}_{\mu\nu} \longrightarrow \underline{t}\cdot \underline{F}'_{\mu\nu} = U \underline{t}\cdot \underline{F}_{\mu\nu} U^+$$

Note that

$$Tr\,(t^A t^B) = \tfrac{1}{2}\delta_{AB}$$

so that

$$Tr\,(\underline{t}\cdot \underline{F}_{\mu\nu}\ \underline{t}\cdot \underline{F}^{\mu\nu}) = Tr\,(t^A F^A_{\mu\nu}\ t^B F^{B\mu\nu})$$
$$= \tfrac{1}{2} F^A_{\mu\nu} F^{A\mu\nu}$$

* Thus

$$F^A_{\mu\nu}\, F^{A\mu\nu} \longrightarrow F'^A_{\mu\nu}\, F'^{A\mu\nu}$$

$$F'^A_{\mu\nu}\, F'^{A\mu\nu} = 2\,\mathrm{Tr}\left(U \underline{t}^A F_{\mu\nu} U^+ U \underline{t}^A F^{\mu\nu} U^+\right)$$

$$= 2\,\mathrm{Tr}\left(\underbrace{U^+U}_{=\mathbb{1}} \underline{t}^A F_{\mu\nu} \underbrace{U^+U}_{=\mathbb{1}} \underline{t}^A F^{\mu\nu}\right)$$

$$= F^A_{\mu\nu}\, F^{A\mu\nu}$$

This confirms that the QCD Lagrangian is invariant w.r.t. SU(3) gauge transformations.

* In addition to quark-gluon couplings

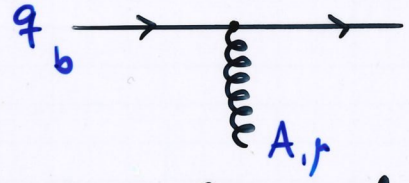

$$-i g_s (t^A)_{cb}\, \gamma^\rho$$

there are also gluon self-couplings

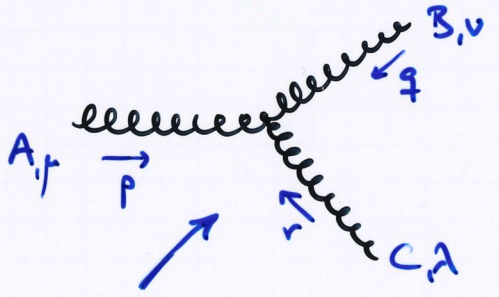

$$-g_s f^{ABC}\left[g^{\mu\nu}(p-q)^\lambda + g^{\nu\lambda}(q-r)^\mu + g^{\lambda\mu}(r-p)^\nu\right]$$

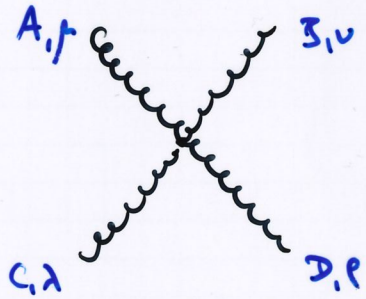

$$-ig_s^2 \cdot \left[f^{XAC} f^{XBD}\left(g_{\mu\nu}g_{\lambda\rho} - g_{\mu\rho}g_{\nu\lambda}\right) + f^{XAD} f^{XBC}\left(g_{\mu\nu}g_{\lambda\rho} - g_{\mu\lambda}g_{\nu\rho}\right) + f^{XAB} f^{XCD}\left(g_{\mu\lambda}g_{\nu\rho} - g_{\mu\rho}g_{\nu\lambda}\right)\right]$$

- Note that gluon field strength tensor is not gauge invariant.
  Contrast this with gauge-invariance of QED field strength. QCD field strength is not gauge invariant because of self-interaction of gluons. Carriers of the colour force are themselves coloured, unlike the electrically neutral photon.

- Note there is no gauge-invariant way of including a gluon mass. A term such as

$$m^2 \mathcal{A}^\alpha \mathcal{A}_\alpha$$

  is not gauge invariant. This is similar to QED result for mass of the photon. On the other hand quark mass term is gauge invariant.

* In addition to $\bar{q}_f q_{f'}$ systems (mesons), there is another class of gauge-invariant systems of quarks:

$$\varepsilon_{abc}\, q_a q_b q_c \longrightarrow \varepsilon_{abc}\, q_a' q_b' q_c'$$
$$= \varepsilon_{abc}\, U_{aa'} U_{bb'} U_{cc'}\, q_{a'} q_{b'} q_{c'}$$
$$= \varepsilon_{a'b'c'} \det U\; q_{a'} q_{b'} q_{c'}$$
$$= \varepsilon_{abc}\, q_a q_b q_c$$

since $\det U = +1$ for any $SU(3)$ matrix.

* Similarly,

$$\varepsilon_{abc}\, \bar{q}_a \bar{q}_b \bar{q}_c \longrightarrow \varepsilon_{abc} \underbrace{\det U^+}_{=1} \bar{q}_a \bar{q}_b \bar{q}_c$$

We recognize these systems as the baryon and antibaryon systems.

* The above meson and baryon states are only invariant w.r.t. local gauge transformations if all the quark and antiquark fields are at the same point. Otherwise, gauge transformation gives

$$\bar{q}(y)\, q(x) \longrightarrow \bar{q}(y) U^+(y)\, U(x) q(x) \neq \bar{q}(y)\, q(x)$$

since in general $U(x) \neq U(y)$ for $x \neq y$.

* To restore gauge invariance we need to introduce the gluon field. This is done with the colour string operator

$$S(y,x) = \mathcal{P} \exp\left[-ig_s \int_x^y dz^\mu \, \underline{t} \cdot \underline{A}_\mu(z)\right]$$

$$= \prod_{z=x}^{y} \left(1 - ig_s \, dz^\mu \, \underline{t} \cdot \underline{A}_\mu(z)\right)$$

where $\mathcal{P}$ stands for path ordering of the matrix product.

* Under gauge transformations

$$1 - ig_s \, dz^\mu \, \underline{t} \cdot \underline{A}_\mu(z) \rightarrow$$

$$\rightarrow 1 - ig_s \, dz^\mu \left[U(z) \underline{t} \cdot \underline{A}_\mu U^+(z) + \frac{i}{g_s} \left(\partial_\mu U(z)\right) U^+(z)\right]$$

$$= \left[U(z) + dz^\mu \partial_\mu U(z)\right]\left[1 - ig_s \, dz^\mu \, \underline{t} \cdot \underline{A}_\mu(z)\right] U^+(z)$$

$$= U(z+dz)\left[1 - ig_s \, dz^\mu \, \underline{t} \cdot \underline{A}_\mu(z)\right] U^+(z)$$

and therefore

$$S(y,x) \rightarrow U(y) \, S(y,x) \, U^+(x) .$$

* Hence the gauge invariant object is a quark and an antiquark joined by a colour string.

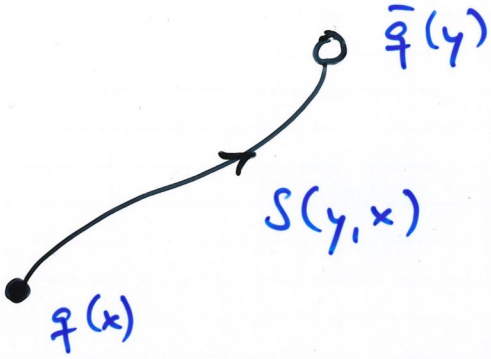

$$\bar{q}(y)\, S(y,x)\, q(x) \rightarrow \bar{q}(y)\, U^{+}(y)\, U(y)\, S(y,x)\, U^{+}(x)\, U(x)\, q(x)$$
$$= \bar{q}(y)\, S(y,x)\, q(x)$$

* This is similar to QED, where the field between an electron and a positron can be regarded as a superposition of strings representing flux lines.

* However, the gauge invariant baryon state has no analogue in QED, since it involves a string junction at some (arbitrary) space-time point w^μ

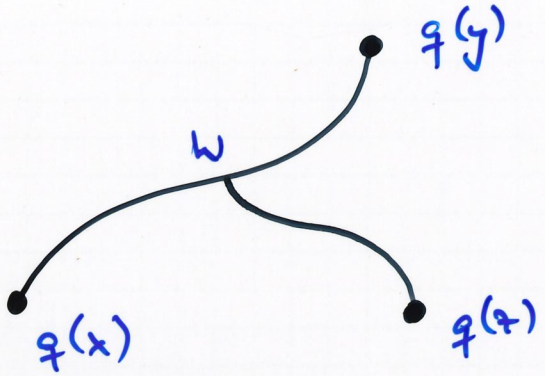

Putting in colour indices explicitly, this is

$$\varepsilon_{abc}\, S_{aa'}(w,x)\, q_{a'}(x)\, S_{bb'}(w,y)\, q_{b'}(y)\, S_{cc'}(w,z)\, q_{c'}(z)$$

which is gauge invariant, by the argument used above for three quarks at the same point.

- In the last years, also a number of tetraquark and pentaquark states have been discovered.
  Tetraquarks consist of four quarks: two quarks and two antiquarks, giving baryon number zero.
  Pentaquarks consist of five quarks: four quarks and one antiquark, giving baryon number one.
  So far, all known tetraquarks and pentaquarks contain at least one heavy quark (charm or bottom). Their internal structure (molecules?) is not yet well understood.

* The force between two colour charges (e.g. quarks) becomes strong at large distances, and is believed to give rise to a linear potential. → 

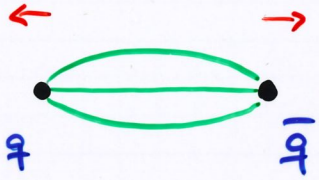

→ 

Quarks (and gluons) can not be observed as isolated objects and exist only in bound states (mesons, baryons). This mechanism is called <u>confinement</u>.

- The force between two colour charges (e.g. quarks) becomes strong at large distances, and is believed to give rise to a linear potential.

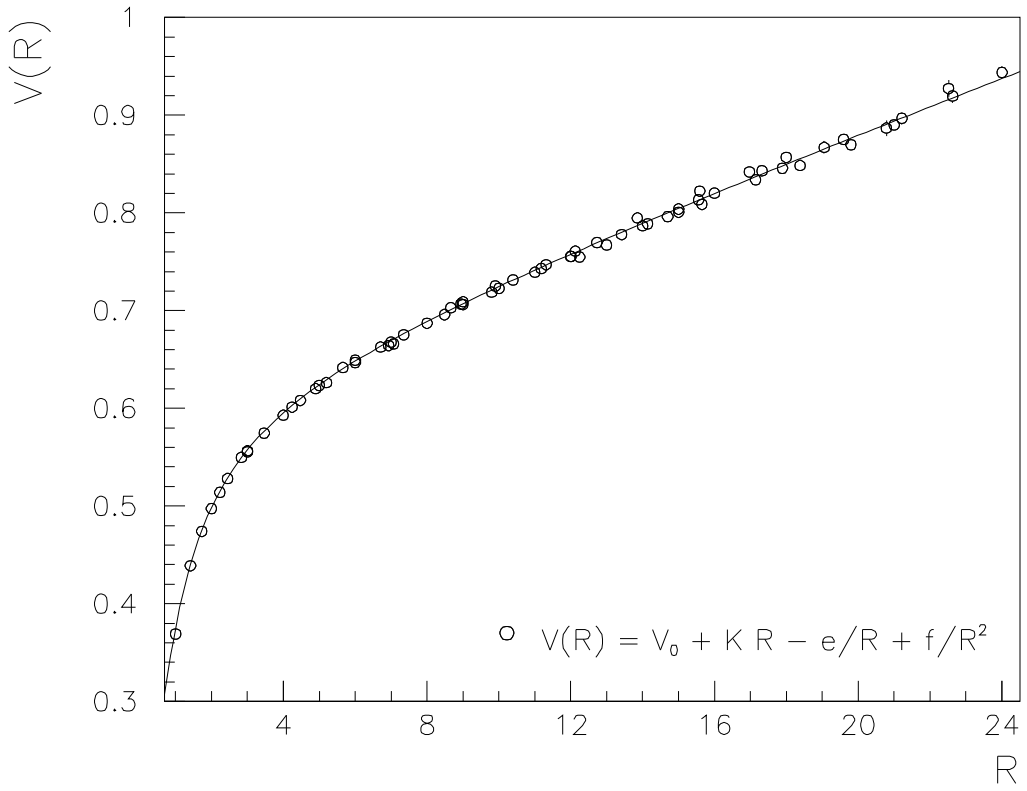

Exact symmetries of QCD

- In addition to being gauge invariant, QCD Lagrangian is invariant under C, P and T transformations.

- A CP violating term could be added to the the QCD Lagrangian, the θ term

$$\mathcal{L}_\theta = \theta \frac{g_s^2}{32\pi^2} F^A_{\mu\nu} \tilde{F}^{A\,\mu\nu}$$

with the dual field strength tensor

$$\tilde{F}^{\mu\nu} = \frac{1}{2} \varepsilon^{\mu\nu\rho\sigma} F_{\rho\sigma}$$

A non-zero value of the parameter θ would imply CP violation. It produces electric dipole moment of neutron. Non-observation of the latter gives limit $\theta \leq 10^{-10}$. No convincing mechanism for absense of θ-term has been found so far. This is the strong CP problem.

Approximate symmetries

- The small difference between u and d quark masses gives rise to an approximate light quark flavour symmetry. Write

$$q = \begin{pmatrix} u \\ d \end{pmatrix}$$

then QCD Lagrangian becomes

$$\mathcal{L} = \bar{q}(i\not{D} + M)q \qquad \text{with} \qquad M = \begin{pmatrix} m_u & 0 \\ 0 & m_d \end{pmatrix}$$

With $m_u - m_d$ much smaller than hadronic mass scales approximate M by diagonal matrix. Then symmetry of $\mathcal{L}$ is increased to $\mathrm{U}(2)_V = \mathrm{U}(1)_V \otimes \mathrm{SU}(2)_V$,

$$q \;\rightarrow\; q' = \exp\left(\sum_0^3 \alpha_i \sigma^i\right) q$$

The new approximate $\mathrm{SU}(2)_V$ symmetry is isospin symmtery (the $\mathrm{U}(1)_V$ symmetry corresponds to quark number conservation).

- ⋆ This symmetry is further enhanced by assuming also the strange quark to be degenerate in mass with the u and d quarks. That gives rise to $\mathrm{SU}(3)_V$ flavour symmetry which gives classification of mesons and baryons into flavour octets and decuplets.
- ⋆ In the limit that u and d quark masses vanish, $M = 0$, symmetry becomes even larger. Introducing left- and right-handed components,

$$q_L = \frac{1}{2}(1 - \gamma_5)q \qquad q_R = \frac{1}{2}(1 + \gamma_5)q$$

quark sector of the Lagrangian is

$$\mathcal{L} = \bar{q}_L i \not{D} q_L + \bar{q}_R i \not{D} q_R$$

Without the mass term positive and negative helicity states are not connected. Therefore independent rotations of the two are permitted, yielding $\mathrm{U}(2)_L \otimes \mathrm{U}(2)_R$ symmetry. A symmetry acting separately on left- and right-handed fields is a chiral symmetry . Here we have a chiral $\mathrm{SU}(2)$. This is again enhanced to chiral $\mathrm{SU}(3)$ if also $m_s = 0$ is assumed.

- ⋆ Chiral symmetry is not apparent in the hadron spectrum (since it would imply a partner with equal mass and opposite parity for every hadron). Instead, chiral SU(2) is spontaneously broken, leaving $\mathrm{SU}(2)_V \otimes \mathrm{U}(1)_V$ as above.
  Spontaneous symmetry breaking takes place if the vacuum state is not invariant under the full symmetry group. The QCD vacuum is believed to be have a nonvanishing expectation value of the light-quark operator $\bar{q}q$,

$$\langle 0|\bar{q}q|0\rangle = \langle 0|(\bar{u}u + \bar{d}d)|0\rangle \simeq (250\,\mathrm{MeV})^3$$

  referred to as a quark condensate. It breaks chiral symmetry since it connects left- and right-handed fields, $\bar{q}q = \bar{q}_L q_R + \bar{q}_R q_L$.
- ⋆ Spontaneous chiral symmetry breaking gives rises to three pseudoscalar Goldstone bosons $\pi^{\pm}, \pi^0$.
  Also $\mathrm{U}(1)_L \otimes \mathrm{U}(1)_R$ is broken down to $\mathrm{U}(1)_V$, but the lost $\mathrm{U}(1)_A$ does not give rise to Goldstone bosons due to quantum effects.
- ⋆ Since light quark masses are not exactly zero also Goldstone bosons are not massless, but still much lighter than all other hadrons. Deviation of light quark masses from zero can be treated as a perturbation, giving rise to chiral perturbation theory.

- ⋆ Neglecting also strange quark mass yields chiral $\mathrm{SU}(3)$, spontaneously broken to $\mathrm{SU}(3)_V$, with eight pseudoscalar Goldstone bosons $\pi^{\pm}, \pi^0, K^{\pm}, K^0, \bar{K}^0, \eta$ corresponding to flavour octet.

- QCD also has approximate heavy quark symmetry which resembles the weak dependence of atoms on the isotopic composition of the nucleus. Heavy quark symmetry relates bound states of c and b quarks. The top quark decays too quickly to form hadronic bound states.

Running Couplings

* In QED the observed electron charge is distance-dependent due to vacuum polarization.

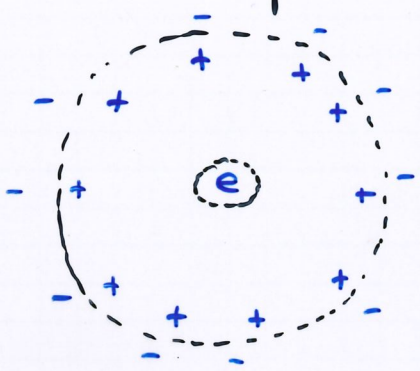

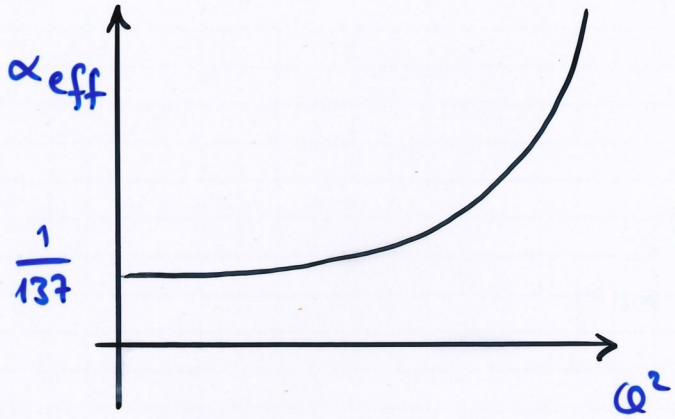

The 1-loop vacuum polarization diagram

is log-divergent and can be regularized by introducing a cut-off Λ. Then

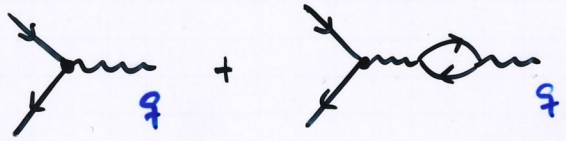

gives

$$\alpha(q^2) = \alpha_{bare}\left(1 + \frac{\alpha}{3\pi}\ln\frac{q^2}{\Lambda^2}\right)$$

Thus

$$q^2\frac{\partial\alpha}{\partial q^2} = \frac{\alpha^2}{3\pi} + \ldots \equiv \beta_{QED}(\alpha)$$

In QED $\beta_{QED}(\alpha) > 0$. ← QED β-function

Therefore $\alpha \to \infty$ at short distances.

* In QCD there is an additional diagram:

As a consequence, the β-function changes. Now

$$\alpha_s(q^2) = \alpha_{s,\text{bare}}\left(1 + \frac{N_f}{6\pi}\alpha_s \ln\frac{q^2}{\Lambda^2} - \frac{11}{4\pi}\alpha_s \ln\frac{q^2}{\Lambda^2} - \dots\right)$$

where N_f is the number of quark flavours. Hence

$$\beta_{QCD}(\alpha_s) = -\beta_0 \alpha_s^2 - \dots < 0$$

!

where

$$\beta_0 = \frac{1}{12\pi}(33 - 2N_f)$$

* The gluonic contribution to the vacuum polarization reverses the sign of the β-function, so that the strong coupling α_s decreases at large q^2 (short distances). This is called asymptotic freedom. It implies that quarks behave as (almost) free particles at short distances, and perturbation theory can be used for hard processes, i.e. processes involving large momentum transfer.

* From

$$q^2 \frac{\partial \alpha_s}{\partial q^2} = \beta(\alpha_s)$$

we find

$$\int_{\alpha_s(\mu^2)}^{\alpha_s(Q^2)} \frac{d\alpha_s}{\beta(\alpha_s)} = \int_{\mu^2}^{Q^2} \frac{dq^2}{q^2} = \ln \frac{Q^2}{\mu^2}$$

In lowest order $\beta(\alpha_s) = -\beta_0 \alpha_s^2$ and thus

$$\frac{1}{\alpha_s(Q^2)} - \frac{1}{\alpha_s(\mu^2)} = \beta_0 \ln \frac{Q^2}{\mu^2}$$

$$\rightarrow \quad \boxed{\alpha_s(Q^2) = \frac{\alpha_s(\mu^2)}{1 + \alpha_s(\mu^2)\beta_0 \ln Q^2/\mu^2}}$$

* We had to introduce a dimensionful parameter (μ) to specify the boundary conditions. Alternatively, define Λ^2_{QCD} as the scale at which solution diverges:

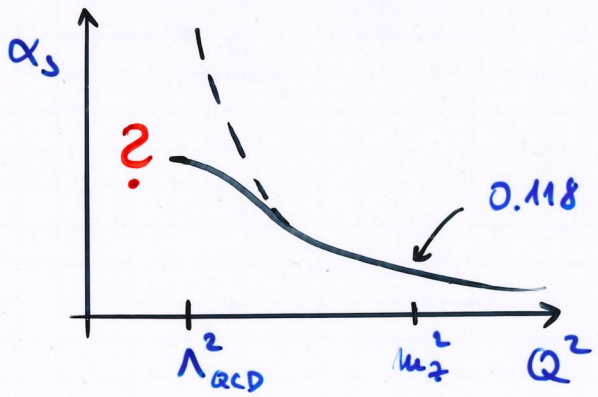

$$\frac{1}{\alpha_s(Q^2)} - 0 = \beta_0 \ln \frac{Q^2}{\Lambda^2_{QCD}}$$

$$\boxed{\alpha_s(Q^2) = \frac{1}{\beta_0 \ln Q^2/\Lambda^2_{QCD}}}$$

* Experimentally, the fundamental scale of QCD is $\Lambda_{QCD} \simeq 210 \pm 40$ MeV.

↑ not to be confused with the cutoff Λ above!

- Nowadays, most calculations are performed in *modified minimal subtraction* ($\overline{\text{MS}}$) renormalization scheme. Ultraviolet divergences are 'dimensionally regularized' by reducing number of space-time dimensions to $D < 4$:

$$\frac{\mathrm{d}^4 k}{(2\pi)^4} \longrightarrow (\mu)^{2\epsilon} \frac{\mathrm{d}^{4-2\epsilon} k}{(2\pi)^{4-2\epsilon}}$$

where $\epsilon = 2 - \frac{D}{2}$. Note that renormalization scale μ still has to be introduced to preserve dimensions of couplings and fields.

- Loop integrals of form

$$\int \frac{\mathrm{d}^D k}{(k^2 + m^2)^2}$$

lead to poles at $\epsilon = 0$. The *minimal subtraction* (MS) prescription is to subtract poles and replace bare coupling by renormalized coupling $\alpha_s(\mu)$. In practice poles always appear in combination

$$\frac{1}{\epsilon} + \ln(4\pi) - \gamma_E,$$

(Euler's constant $\gamma_E = 0.5772\ldots$). In *modified* minimal subtraction scheme

$\ln(4\pi) - \gamma_E$ is subtracted as well. It follows that

$$\Lambda_{\overline{\text{MS}}} = \Lambda_{\text{MS}} e^{[\ln(4\pi)-\gamma_E]/2} = 2.66\,\Lambda_{\text{MS}}$$

- Current best fit value of α_s at mass of Z is

$$\alpha_s(M_Z) = 0.1179 \pm 0.0010$$

corresponding to a preferred value of $\Lambda_{\overline{\text{MS}}}$ (for $N_f = 5$) in the range

$$196 \text{ MeV} < \Lambda^{(5)}_{\overline{\text{MS}}} < 224 \text{ MeV}.$$

- Uncertainty in α_s propagates directly into QCD cross sections. Thus we expect at least errors of $\sim 1\%$ in prediction of cross sections which begin in order α_s.

- Recent compilation of α_s measurements is shown below. Evidence that $\alpha_s(Q)$ has a logarithmic fall-off with Q is persuasive.

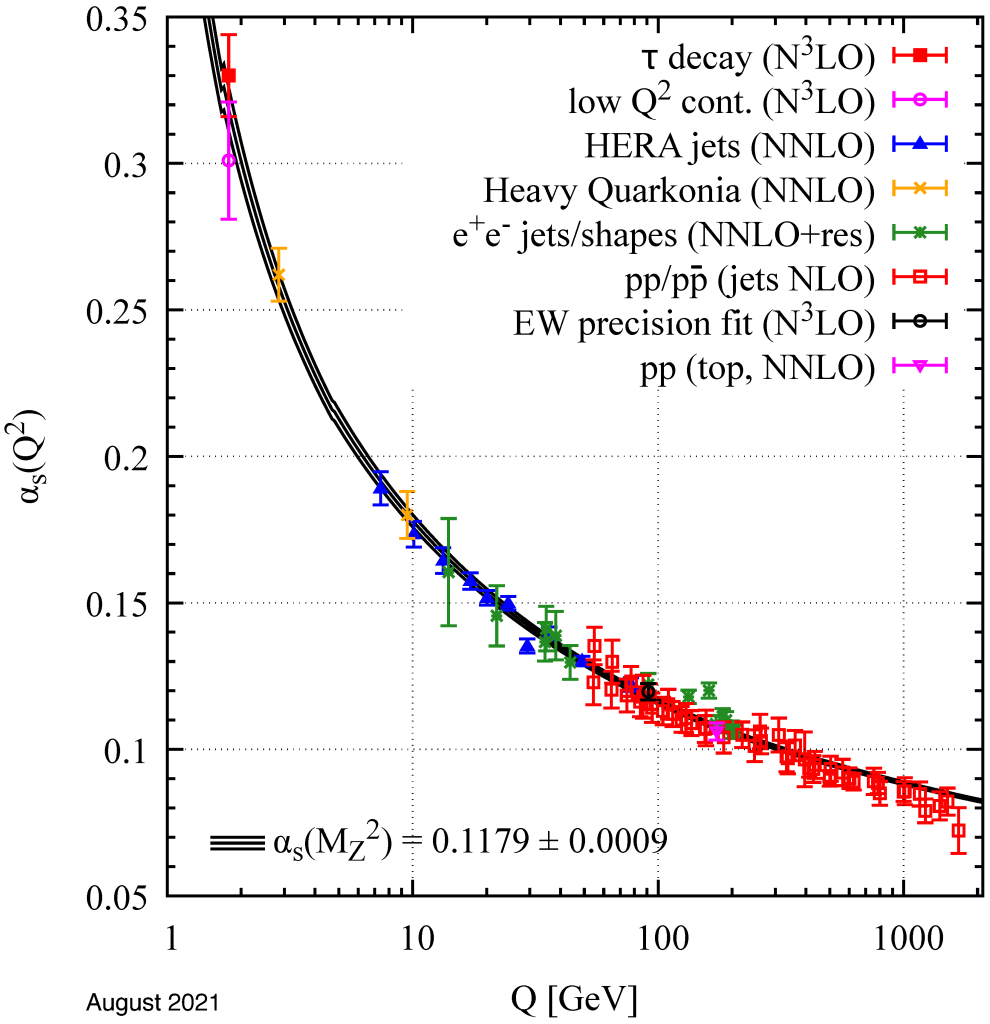

- Using the formula for running $\alpha_s(Q)$ to rescale all measurements to $Q = M_Z$ gives excellent agreement.

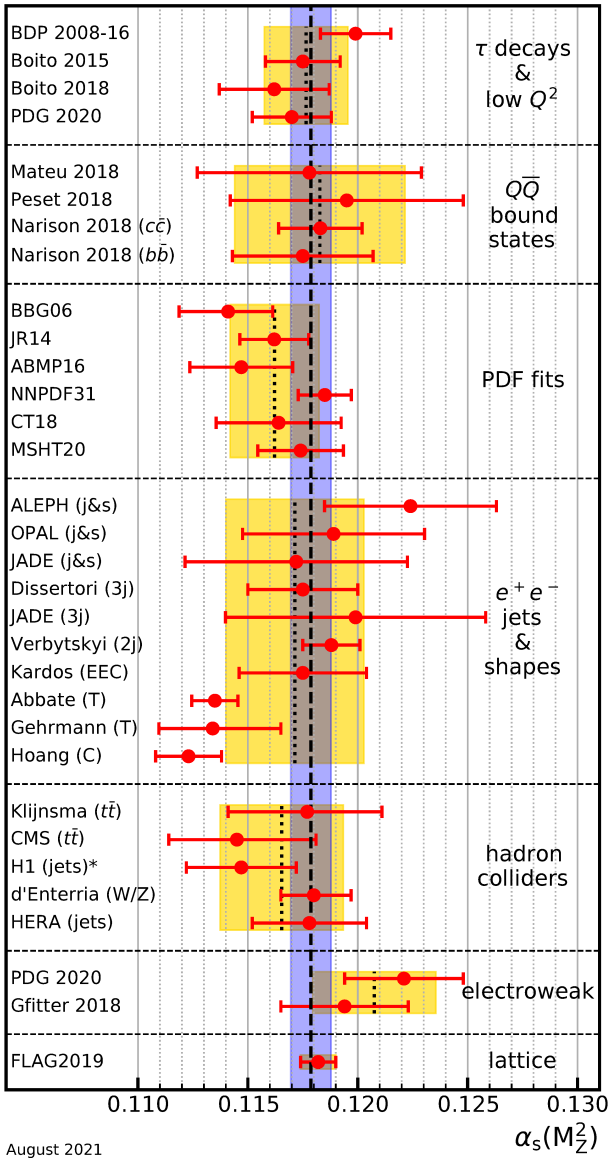

Nonperturbative QCD

* Corresponding to asymptotic freedom at high momentum scales (short distances) we have **infrared slavery**: $\alpha_s(Q^2)$ becomes large at low momenta (long distances). Perturbation theory (PT) not reliable for large α_s, so nonperturbative methods (**lattice QCD**, ...) must be used.

  ↳ see later

* Important low momentum-scale phenomena:
  * **Confinement**: partons (quarks and gluons) found only in color-singlet bound states (hadrons), size ~ 1 fm.
  * **Hadronization**: partons produced in short-distance interactions reorganize themselves (and multiply) to make observed hadrons.

* Note that confinement is a static (long distance) property of QCD, treatable by lattice techniques, whereas hadronization is a dynamical (long timescale) phenomenon: only models are available at present.

* The main idea behind hadronization models is local parton-hadron duality: hadronization involves small momentum transfers. Hence hadron-level flow of energy-momentum, flavour should follow parton level. In fact, results on spectra and multiplicities support this.

* For the details of hadron formation one needs specific models. Main current models are cluster and string.

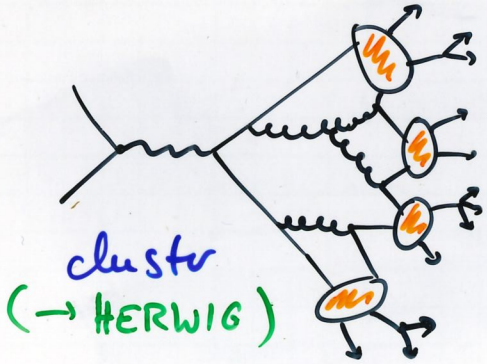

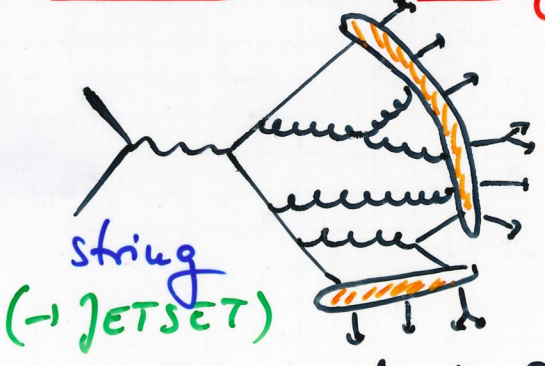

These models are implemented in Monte Carlo simulations.

Infrared divergences

- Even in high-energy, short-distance regime, long-distance aspects of QCD cannot be ignored. Soft or collinear gluon emission gives infrared divergences in PT. Light quarks ($m_q \ll \Lambda$) also lead to divergences in the limit $m_q \to 0$ (mass singularities).

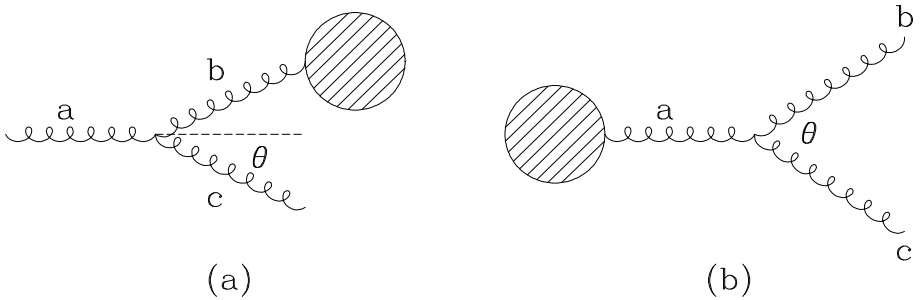

  - ⋆ Spacelike branching: gluon splitting on incoming line (a)

$$p_b^2 = -2E_a E_c(1-\cos\theta) \le 0 \; .$$

Propagator factor $1/p_b^2$ diverges as $E_c \to 0$ (soft singularity) or $\theta \to 0$ (collinear or mass singularity). If a and b are quarks, inverse propagator factor is

$$p_b^2 - m_q^2 = -2E_a E_c(1-v_a\cos\theta) \le 0 \; ,$$

Hence $E_c \to 0$ soft divergence remains; collinear enhancement becomes a divergence as $v_a \to 1$, i.e. when quark mass is negligible. If emitted parton c is a quark, vertex factor cancels $E_c \to 0$ divergence.

⋆ Timelike branching: gluon splitting on outgoing line (b)

$$p_a^2 = 2E_bE_c(1 - \cos\theta) \geq 0 \; .$$

Diverges when either emitted gluon is soft (E_b or $E_c \to 0$) or when opening angle $\theta \to 0$. If b and/or c are quarks, collinear/mass singularity in $m_q \to 0$ limit. Again, soft quark divergences cancelled by vertex factor.

- Similar infrared divergences in loop diagrams, associated with soft and/or collinear configurations of virtual partons within region of integration of loop momenta.

- Infrared divergences indicate dependence on long-distance aspects of QCD not correctly described by PT. Divergent (or enhanced) propagators imply propagation of partons over long distances. When distance becomes comparable with hadron size ~ 1 fm, quasi-free partons of perturbative calculation are confined/hadronized non-perturbatively, and apparent divergences disappear.

- Can still use PT to perform calculations, provided we limit ourselves to two classes of observables:
  - ⋆ Infrared safe quantities, i.e. those insensitive to soft or collinear branching. Infrared divergences in PT calculation either cancel between real and virtual contributions or are removed by kinematic factors. Such quantities are determined primarily by hard, short-distance physics; long-distance effects give power corrections, suppressed by inverse powers of a large momentum scale.
  - ⋆ Factorizable quantities, i.e. those in which infrared sensitivity can be absorbed into an overall non-perturbative factor, to be determined experimentally.

- In either case, infrared divergences must be *regularized* during PT calculation, even though they cancel or factorize in the end.
  - ⋆ Gluon mass regularization: introduce finite gluon mass, set to zero at end of calculation. However, as we saw, gluon mass breaks gauge invariance.
  - ⋆ Dimensional regularization: analogous to that used for ultraviolet divergences, except we must *increase* dimension of space-time, $\epsilon = 2 - \frac{D}{2} < 0$. Divergences are replaced by powers of $1/\epsilon$.

e^+e^- annihilation cross section

- $e^+e^- \to \mu^+\mu^-$ is fundamental electroweak process. The same type of process, $e^+e^- \to q\bar{q}$, will produce hadrons. Cross sections are roughly proportional.

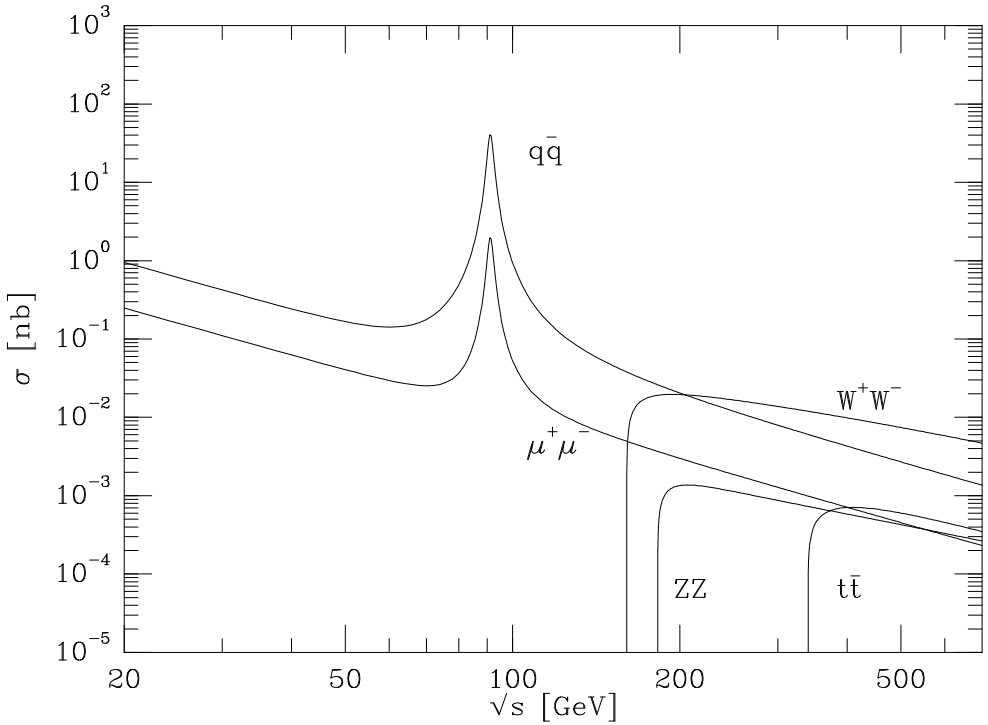

- But formation of hadrons is a non-perturbative process. How can PT give correct hadronic cross section? To understand this visualize event in space-time:

  ⋆ e^+ and e^- collide to form γ or Z^0 with virtual mass $Q = \sqrt{s}$. This fluctuates into $q\bar{q}$, $q\bar{q}g$, . . . , occupying space-time volume $\sim 1/Q$. At large Q, rate for this short-distance process is given by PT.

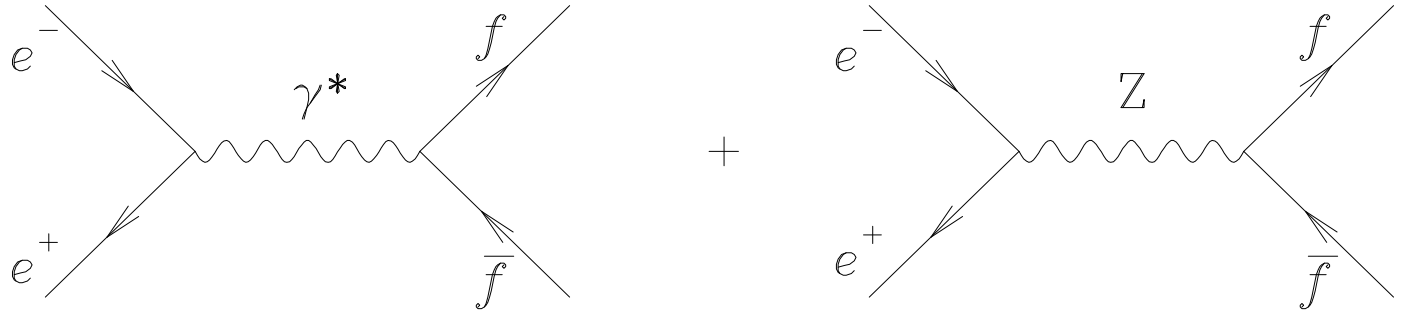

  ⋆ Subsequently, at much later time $\sim 1/\Lambda$, produced quarks and gluons form hadrons. This modifies outgoing state, but occurs too late to change original probability for event to happen.

- Well below Z^0 mass, process $e^+e^- \to f\bar{f}$ is purely electromagnetic, with lowest-order (Born) cross section (neglecting quark masses)

$$\sigma_0 = \frac{4\pi\alpha^2}{3s} Q_f^2$$

Thus ($N = 3 =$ possible number of $q\bar{q}$ colors)

$$R \equiv \frac{\sigma(e^+e^- \to \text{hadrons})}{\sigma(e^+e^- \to \mu^+\mu^-)} = \frac{\sum_q \sigma(e^+e^- \to q\bar{q})}{\sigma(e^+e^- \to \mu^+\mu^-)} = 3\sum_q Q_q^2 \,.$$

- On Z^0 pole, $\sqrt{s} = M_Z$, neglecting γ/Z interference

$$\sigma_0 = \frac{4\pi\alpha^2\kappa^2}{3\Gamma_Z^2}\,(a_e^2 + v_e^2)(a_f^2 + v_f^2)$$

where $\kappa = \sqrt{2}G_F M_Z^2/4\pi\alpha = 1/\sin^2(2\theta_W) \simeq 1.5$. Hence

$$R_Z = \frac{\Gamma(Z \to \text{hadrons})}{\Gamma(Z \to \mu^+\mu^-)} = \frac{\sum_q \Gamma(Z \to q\bar{q})}{\Gamma(Z \to \mu^+\mu^-)} = \frac{3\sum_q (a_q^2 + v_q^2)}{a_\mu^2 + v_\mu^2}$$

- Measured cross section is about 5% higher than σ_0 due to QCD corrections. For massless quarks, corrections to R and R_Z are equal. To $\mathcal{O}(\alpha_s)$ we have the diagrams

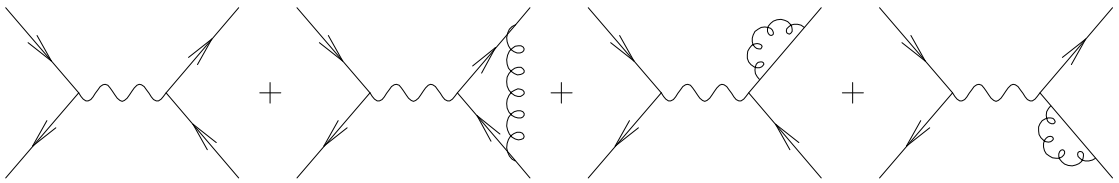

(a)

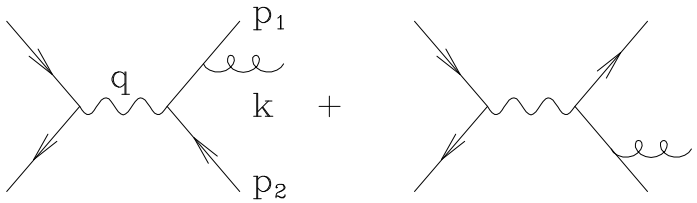

(b)

- Real emission diagrams (b) contain soft ($E_g \to 0$) and collinear ($\theta_{qg} \to 0$ or $\theta_{\bar{q}g} \to 0$) divergences. These singularities are not physical – they simply indicate the breakdown of PT when energies and / or invariant masses approach QCD scale $\Lambda_{\rm QCD}$.

- Collinear and/or soft regions do not make important contribution to R. To see this, make integrals finite using dimensional regularization, $D = 4 - 2\epsilon$, but $\epsilon < 0$ now.

Then

$$\sigma^{q\bar{q}g} = 2\sigma_0 \frac{\alpha_s}{\pi} H(\epsilon) \left[\frac{2}{\epsilon^2} + \frac{3}{\epsilon} + \frac{19}{2} - \pi^2 + \mathcal{O}(\epsilon) \right]$$

with

$$H(\epsilon) = \frac{3(1-\epsilon)(4\pi)^{2\epsilon}}{(3-2\epsilon)\Gamma(2-2\epsilon)} = 1 + \mathcal{O}(\epsilon)$$

Now soft and collinear singularities are regulated and appear as poles at $D = 4$.

- Virtual gluon contributions, diagrams (a), give in dimensional regularization

$$\sigma^{q\bar{q}} = 3\sigma_0 \left\{ 1 + \frac{2\alpha_s}{3\pi} H(\epsilon) \left[-\frac{2}{\epsilon^2} - \frac{3}{\epsilon} - 8 + \pi^2 + \mathcal{O}(\epsilon) \right] \right\}$$

- Adding real and virtual contributions, poles cancel and result is finite as $\epsilon \to 0$:

$$R = 3 \sum_q Q_q^2 \left[1 + \frac{\alpha_s}{\pi} + \mathcal{O}(\alpha_s^2) \right]$$

Thus R is an infrared safe quantity.

- Coupling constant α_s is evaluated at renormalization scale μ . UV divergences in R cancel to $\mathcal{O}(\alpha_s)$, so coefficient of α_s is independent of μ. At $\mathcal{O}(\alpha_s^2)$ and higher, UV divergences make coefficients renormalization scale and scheme dependent:

$$\begin{aligned} R &= 3\,K_{QCD}\sum_q Q_q^2 \\ K_{QCD} &= 1+\frac{\alpha_s(\mu^2)}{\pi}+\sum_{n\geq 2} C_n\left(\frac{s}{\mu^2}\right)\left(\frac{\alpha_s(\mu^2)}{\pi}\right)^n \end{aligned}$$

- Scale and scheme dependence only cancels completely when series is computed to all orders. A scale change at $\mathcal{O}(\alpha_s^n)$ induces changes at $\mathcal{O}(\alpha_s^{n+1})$. The more terms are added, the more stable is the prediction with respect to changes in μ.

- Residual scale dependence is an important source of uncertainty in QCD predictions. One can vary the scale over some 'physically reasonable' range, e. g. $\sqrt{s}/2 < \mu < 2\sqrt{s}$, to try to quantify this uncertainty. But there is no real substitute for a full higher-order calculation.

- Residual scale dependence:

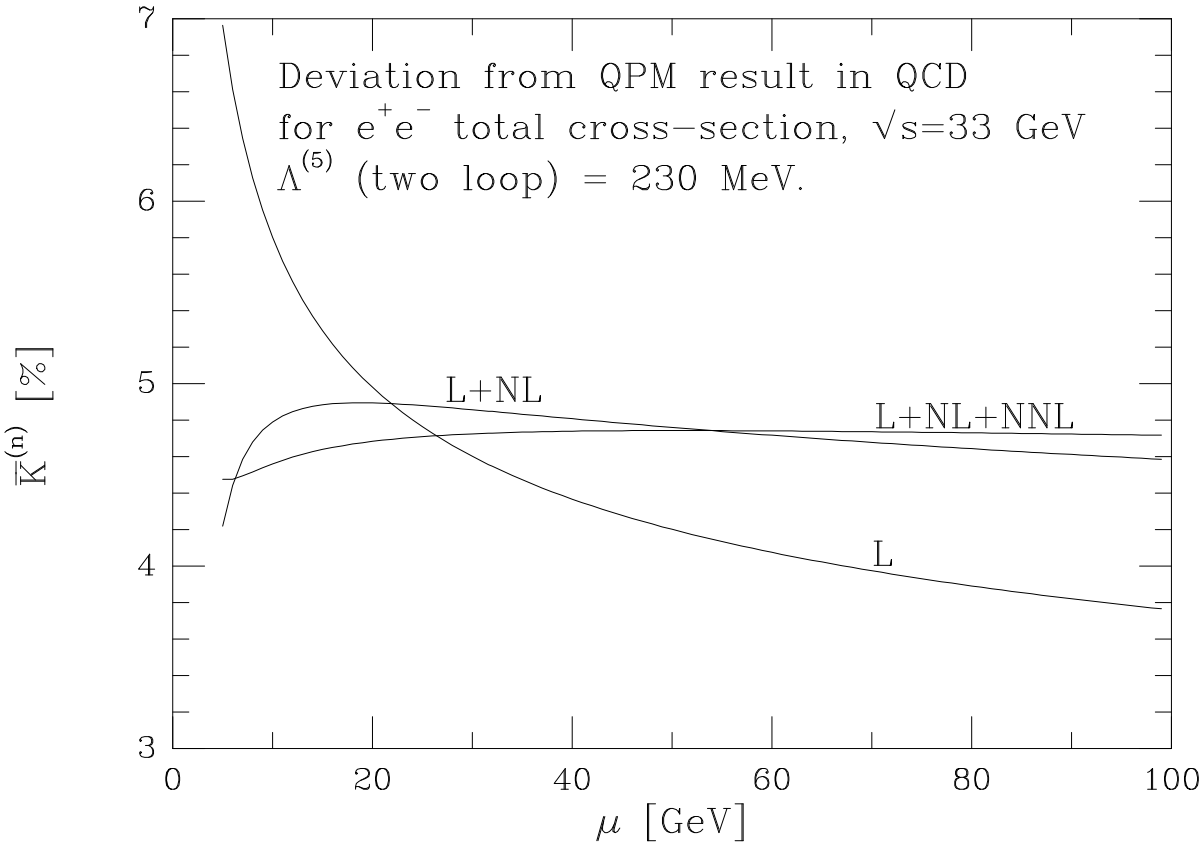

Deep inelastic scattering

- Consider lepton-proton scattering via exchange of virtual photon:

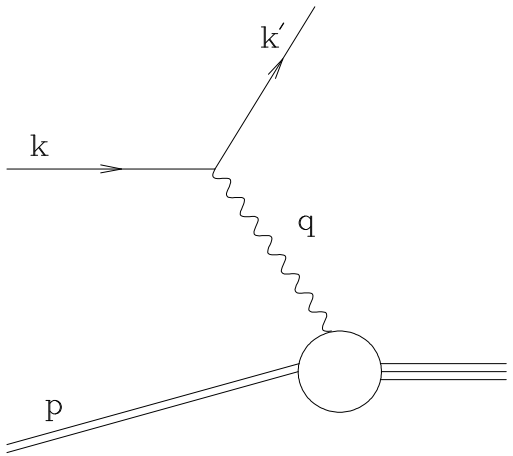

- Standard variables are:

$$x = \frac{-q^2}{2p\cdot q} = \frac{Q^2}{2M(E-E')}$$

$$y = \frac{q\cdot p}{k\cdot p} = 1 - \frac{E'}{E}$$

where $Q^2 = -q^2 > 0$, $M^2 = p^2$ and energies refer to target rest frame.

- Elastic scattering has $(p+q)^2 = M^2$, i.e. $x = 1$. Hence deep inelastic scattering (DIS) means $Q^2 \gg M^2$ and $x < 1$.

- Structure functions $F_i(x, Q^2)$ parametrise target structure as 'seen' by virtual photon. Defined in terms of cross section

$$\frac{d^2\sigma}{dxdy} = \frac{8\pi\alpha^2 ME}{Q^4}\left[\left(\frac{1+(1-y)^2}{2}\right)2xF_1 + (1-y)(F_2 - 2xF_1) - (M/2E)xyF_2\right].$$

- Bjorken limit is $Q^2,\ p\cdot q \to \infty$ with x fixed. In this limit structure functions obey approximate Bjorken scaling law, i.e. depend only on dimensionless variable x:

$$F_i(x, Q^2) \longrightarrow F_i(x).$$

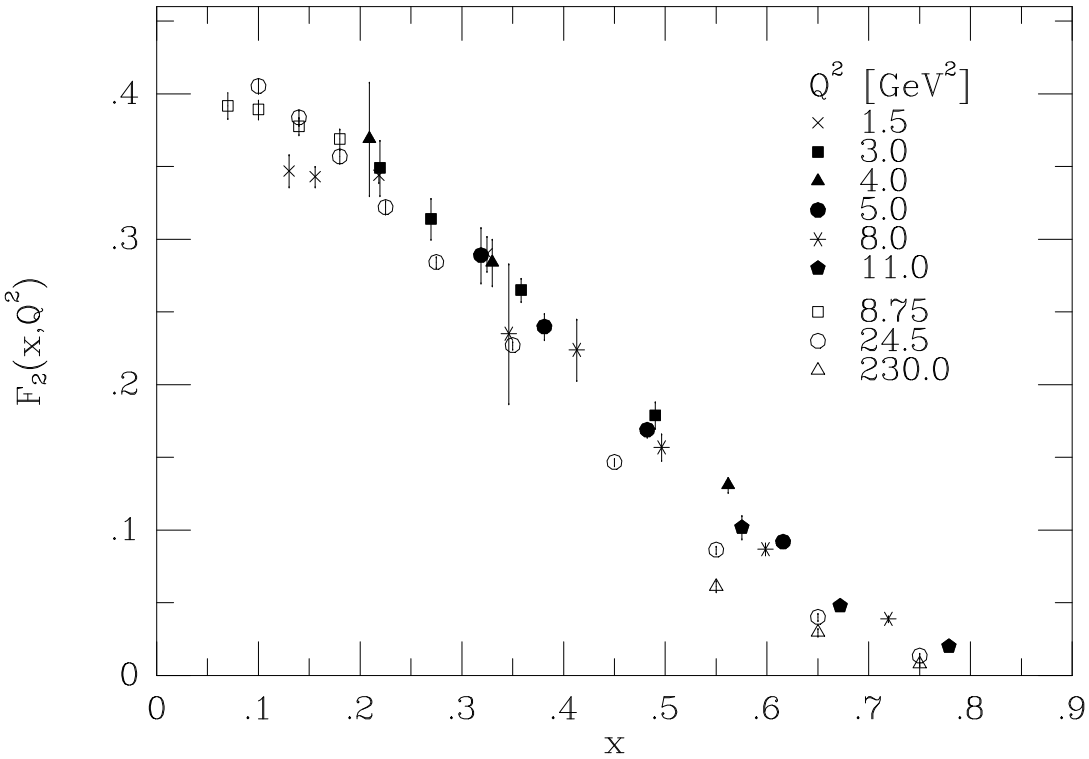

- Figure shows F_2 structure function for proton target. Although Q^2 varies by two orders of magnitude, in first approximation data lie on universal curve.

- Bjorken scaling implies that virtual photon is scattered by *pointlike constituents* (partons) — otherwise structure functions would depend on ratio Q/Q_0, with $1/Q_0$ a length scale characterizing size of constituents.

- Parton model of DIS is formulated in a frame where target proton is moving very fast — *infinite momentum frame*.

  ⋆ Suppose that, in this frame, photon scatters from pointlike quark with fraction ξ of proton's momentum. Since $(\xi p+q)^2 = m_q^2 \ll Q^2$, we must have $\xi = Q^2/2p\cdot q = x$.

  ⋆ In terms of Mandelstam variables $\hat{s}, \hat{t}, \hat{u}$, spin-averaged matrix element squared for massless $eq \to eq$ scattering (related by crossing to $e^+e^- \to q\bar{q}$) is

$$\overline{\sum}|\mathcal{M}|^2 = 2e_q^2 e^4 \frac{\hat{s}^2+\hat{u}^2}{\hat{t}^2}$$

  where $\overline{\sum}$ denotes average (sum) over initial (final) colours and spins.

  ⋆ In terms of DIS variables, $\hat{t} = -Q^2$, $\hat{u} = \hat{s}(y-1)$ and $\hat{s} = Q^2/xy$. Differential cross section is then

$$\frac{d^2\hat{\sigma}}{dxdQ^2} = \frac{4\pi\alpha^2}{Q^4}[1+(1-y)^2]\frac{1}{2}e_q^2\delta(x-\xi).$$

- From structure function definition (neglecting M)

$$\frac{d^2\sigma}{dxdQ^2} = \frac{4\pi\alpha^2}{Q^4}\left\{[1+(1-y)^2]F_1 + \frac{(1-y)}{x}(F_2 - 2xF_1)\right\}.$$

- Hence structure functions for scattering from parton with momentum fraction ξ is

$$\hat{F}_2 = xe_q^2\delta(x-\xi) = 2x\hat{F}_1 \ .$$

- Suppose probability that quark q carries momentum fraction between ξ and $\xi + d\xi$ is $q(\xi)\,d\xi$. Then

$$\begin{aligned} F_2(x) &= \sum_q \int_0^1 d\xi\ q(\xi)\ xe_q^2\delta(x-\xi) \\ &= \sum_q e_q^2 xq(x) = 2xF_1(x)\ . \end{aligned}$$

- Relationship $F_2 = 2xF_1$ (Callan-Gross relation) follows from spin-$\frac{1}{2}$ property of quarks ($F_1 = 0$ for spin-0).

- Proton consists of three valence quarks (uud), which carry its electric charge and baryon number, and infinite sea of light $q\bar{q}$ pairs.

- Probed at scale Q, sea contains all quark flavours with $m_q \ll Q$. Thus at $Q \sim 1$ GeV expect

$$F_2^{em}(x) \simeq \frac{4}{9}x[u(x) + \bar{u}(x)] + \frac{1}{9}x[d(x) + \bar{d}(x) + s(x) + \bar{s}(x)]$$

where

$$\begin{aligned} u(x) &= u_V(x) + \bar{u}(x) \\ d(x) &= d_V(x) + \bar{d}(x) \\ s(x) &= \bar{s}(x) \end{aligned}$$

with sum rules

$$\int_0^1 dx\, u_V(x) = 2\,, \quad \int_0^1 dx\, d_V(x) = 1\,.$$

- Experimentally one finds

$$\sum_q \int_0^1 dx\; x[q(x) + \bar{q}(x)] \simeq 0.5\ .$$

Thus quarks only carry about 50% of proton's momentum. Rest is carried by *gluons*. Although not directly measured in DIS, gluons participate in other hard scattering processes such as large-p_T jet and prompt photon production.

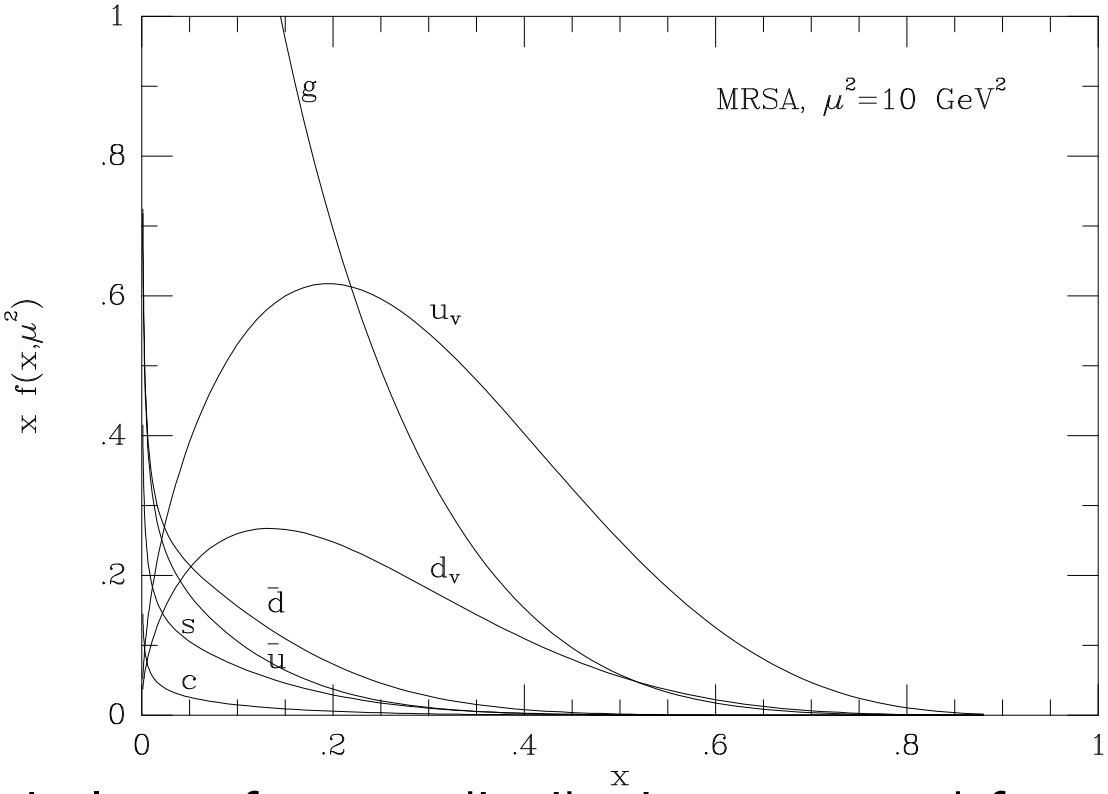

- Figure shows typical set of parton distributions extracted from fits to DIS data, at $Q^2 = 10$ GeV^2.

Parton Branching

* Leading soft and collinear enhanced terms in QCD matrix elements (and corresponding virtual corrections) can be identified and summed to all orders. Consider splitting of outgoing parton a into $b+c$:

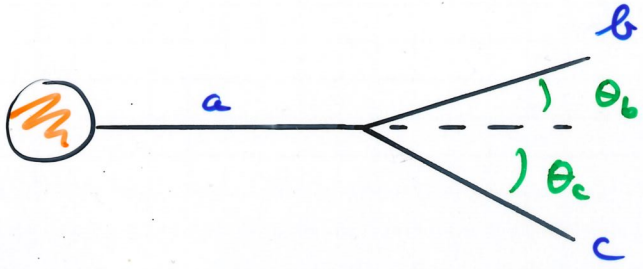

* Can assume $p_b^2, p_c^2 \ll p_a^2 = t$

Opening angle is $\theta = \theta_a + \theta_b$.

Energy fraction of parton b is

$$z = \frac{E_b}{E_a} = 1 - \frac{E_c}{E_a}$$

* For small angles

$$t = 2 E_b E_c (1 - \cos\theta)$$

$$= z(1-z) E_a^2 \theta^2$$

$$\theta = \frac{1}{E_a}\left(\frac{t}{z(1-z)}\right)^{1/2} = \frac{\theta_b}{1-z} = \frac{\theta_c}{z}$$

* Consider first $g \to gg$ branching:

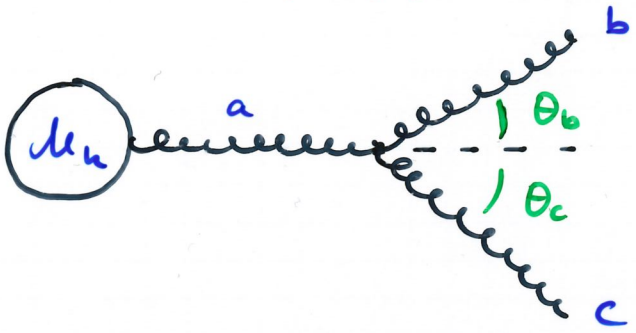

* Matrix element squared for $n+1$ partons is (in small-angle region) given in terms of that for n partons:

$$|M_{n+1}|^2 \sim \frac{4g_s^2}{t} C_A F(z, \varepsilon_a, \varepsilon_b, \varepsilon_c) |M_n|^2$$

with colour factor $C_A = 3$ and ε_i^μ are polarization vectors for gluons $i = a, b, c$.

* Sum / averaging over gluon polarizations gives (with $\langle F \rangle$ the sum / average of F above) in leading order PT calculation

$$\hat{P}_{gg}(z) \equiv C_A \langle F \rangle$$
$$= C_A \left[\frac{1-z}{z} + \frac{z}{1-z} + z(1-z) \right]$$

This is the gluon splitting function.

* Note enhancements due to soft gluons at $z \to 0$ (b soft) and at $z \to 1$ (c soft).

* Consider next $g \to q\bar{q}$ branching:

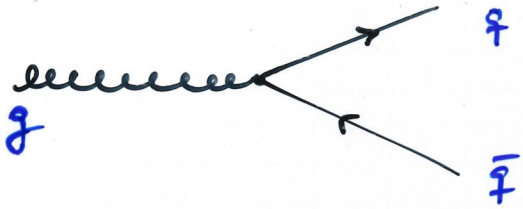

* Here spin-averaged splitting function is

$$\hat{P}_{qg}(z) \equiv T_R \langle F \rangle = T_R \left[z^2 + (1-z)^2 \right]$$

with $T_R = \frac{1}{2}$ from $\mathrm{tr}(t^A t^B) = T_R \delta^{AB}$, and z denotes energy fraction of q.

* No soft ($z \to 0$ or 1) singularities since these are associated only with gluon emission.

* Branching $q \to qg$:

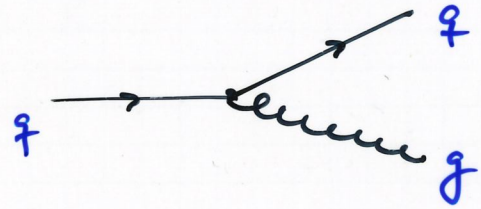

* Spin-averaged splitting function is

$$\hat{P}_{qq}(z) \equiv C_F \langle F \rangle = C_F \frac{1+z^2}{1-z}$$

* Note notation: $\hat{P}_{ba}(z)$ [or $\hat{P}_{b \leftarrow a}(z)$] stands for process $a \to b + c$ with b carrying energy fraction z.

* $\hat{P}_{qg}$ and $\hat{P}_{qq}$ are independent of quark flavour.

Evolution of quark distribution

- Consider enhancement of higher-order contributions due to multiple small-angle parton emission, for example in deep inelastic scattering (DIS)

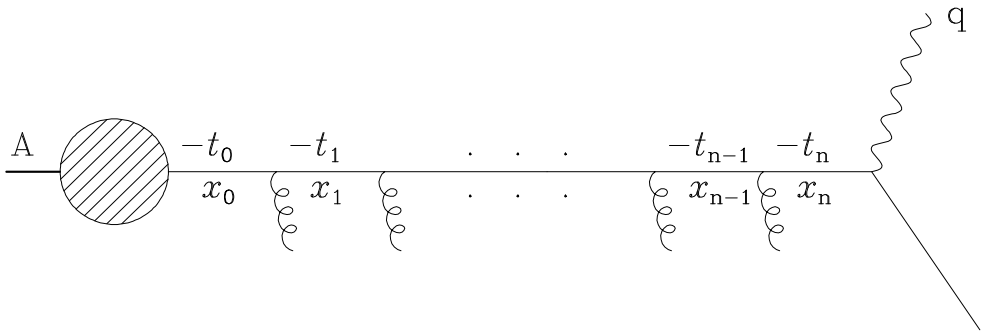

- Incoming quark from target hadron, initially with low virtual mass-squared $-t_0$ and carrying a fraction x_0 of hadron's momentum, moves to more virtual masses and lower momentum fractions by successive small-angle emissions, and is finally struck by photon of virtual mass-squared $q^2 = -Q^2$.

- Cross section will depend on Q^2 and on momentum fraction distribution of partons seen by virtual photon at this scale, $D(x, Q^2)$.

- To derive evolution equation for Q^2-dependence of $D(x, Q^2)$, first introduce pictorial representation of evolution (also useful for Monte Carlo simulation).

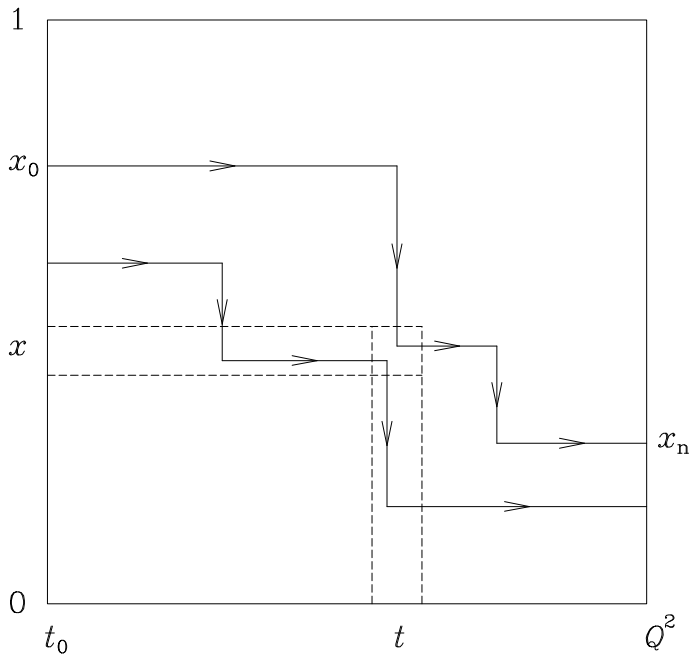

- Represent sequence of branchings by path in (t, x)-space. Each branching is a step downwards in x, at a value of t equal to (minus) the virtual mass-squared after the branching.
- At $t = t_0$, paths have distribution of starting points $D(x_0, t_0)$ characteristic of target hadron at that scale. Then distribution $D(x, t)$ of partons at scale t is just the x-distribution of paths at that scale.
- Consider change in the parton distribution $D(x, t)$ when t is increased to $t + \delta t$. This is number of paths arriving in element $(\delta t, \delta x)$ minus number leaving that element, divided by δx.

- Number arriving is branching probability times parton density integrated over all higher momenta $x' = x/z$,

$$\begin{aligned}\delta D_{\text{in}}(x,t) &= \frac{\delta t}{t}\int_x^1 dx'\,dz\frac{\alpha_s}{2\pi}\hat{P}(z)D(x',t)\,\delta(x-zx') \\ &= \frac{\delta t}{t}\int_0^1 \frac{dz}{z}\frac{\alpha_s}{2\pi}\hat{P}(z)D(x/z,t)\end{aligned}$$

- For the number leaving element, must integrate over lower momenta $x' = zx$:

$$\begin{aligned}\delta D_{\text{out}}(x,t) &= \frac{\delta t}{t}D(x,t)\int_0^x dx'\,dz\frac{\alpha_s}{2\pi}\hat{P}(z)\,\delta(x'-zx) \\ &= \frac{\delta t}{t}D(x,t)\int_0^1 dz\frac{\alpha_s}{2\pi}\hat{P}(z)\end{aligned}$$

- Change in population of element is

$$\begin{aligned}\delta D(x,t) &= \delta D_{\text{in}} - \delta D_{\text{out}} \\ &= \frac{\delta t}{t}\int_0^1 dz\,\frac{\alpha_s}{2\pi}\hat{P}(z)\left[\frac{1}{z}D(x/z,t) - D(x,t)\right]\ .\end{aligned}$$

- Introduce plus-prescription with definition

$$\int_0^1 dz\, f(z)\, g(z)_+ \;=\; \int_0^1 dz\, [f(z) - f(1)]\, g(z)\;.$$

Using this we can define regularized splitting function

$$P(z) = \hat{P}(z)_+\;,$$

and obtain Dokshitzer-Gribov-Lipatov-Altarelli-Parisi (DGLAP) evolution equation:

$$t\frac{\partial}{\partial t} D(x,t) = \int_x^1 \frac{dz}{z}\frac{\alpha_s}{2\pi} P(z) D(x/z,t)\;.$$

- Here $D(x,t)$ represents parton momentum fraction distribution inside incoming hadron probed at scale t. In timelike branching, it represents instead hadron momentum fraction distribution produced by an outgoing parton. Boundary conditions and direction of evolution are different, but evolution equation remains the same.

Quark and gluon distributions

- For several different types of partons, must take into account different processes by which parton of type i can enter or leave the element $(\delta t, \delta x)$. This leads to coupled DGLAP evolution equations of form

$$t\frac{\partial}{\partial t}D_i(x,t) = \sum_j \int_x^1 \frac{dz}{z}\frac{\alpha_s}{2\pi}P_{ij}(z)D_j(x/z,t)\ .$$

- Quark ($i = q$) can enter element via either $q \to qg$ or $g \to q\bar{q}$, but can only leave via $q \to qg$. Thus plus-prescription applies only to $q \to qg$ part, giving

$$\begin{aligned} P_{qq}(z) &= \hat{P}_{qq}(z)_+ = C_F\left(\frac{1+z^2}{1-z}\right)_+ \\ P_{qg}(z) &= \hat{P}_{qg}(z) = T_R\left[z^2+(1-z)^2\right] \end{aligned}$$

- Gluon can arrive either from $g \to gg$ (2 contributions) or from $q \to qg$ (or $\bar{q} \to \bar{q}g$). Thus number arriving is

$$\begin{aligned}
\delta D_{g,\,\text{in}} &= \frac{\delta t}{t}\int_0^1 dz \frac{\alpha_s}{2\pi}\Bigg\{\hat{P}_{gg}(z)\left[\frac{D_g(x/z,t)}{z}+\frac{D_g(x/(1-z),t)}{1-z}\right] \\
&\quad + \frac{\hat{P}_{qq}(z)}{1-z}\left[D_q\left(\frac{x}{1-z},t\right)+D_{\bar{q}}\left(\frac{x}{1-z},t\right)\right]\Bigg\} \\
&= \frac{\delta t}{t}\int_0^1 \frac{dz}{z}\frac{\alpha_s}{2\pi}\left\{2\hat{P}_{gg}(z)D_g\left(\frac{x}{z},t\right)+\hat{P}_{qq}(1-z)\left[D_q\left(\frac{x}{z},t\right)+D_{\bar{q}}\left(\frac{x}{z},t\right)\right]\right\},
\end{aligned}$$

- Gluon can leave by splitting into either gg or $q\bar{q}$, so that

$$\delta D_{g,\,\text{out}} = \frac{\delta t}{t} D_g(x,t)\int_0^1 dz \frac{\alpha_s}{2\pi}\left[\hat{P}_{gg}(z)+N_f\hat{P}_{qg}(z)\,dz\right] .$$

- After some manipulation we find

$$P_{gg}(z) = 2C_A\left[\left(\frac{z}{1-z}+\tfrac{1}{2}z(1-z)\right)_+ + \frac{1-z}{z}+\tfrac{1}{2}z(1-z)\right] - \frac{2}{3}N_f T_R\,\delta(1-z)\,,$$

$$P_{gq}(z) = P_{g\bar{q}}(z) = \hat{P}_{qq}(1-z) = C_F\frac{1+(1-z)^2}{z}\,.$$

- Using definition of the plus-prescription, can show that P_{qq} and P_{gg} can be written in more common forms

$$P_{qq}(z) = C_F\left[\frac{1+z^2}{(1-z)_+}+\frac{3}{2}\delta(1-z)\right]$$

$$P_{gg}(z) = 2C_A\left[\frac{z}{(1-z)_+}+\frac{1-z}{z}+z(1-z)\right]+\frac{1}{6}(11C_A-4N_f T_R)\,\delta(1-z)\,.$$

* The leading-order DLAP splitting functions $P_{ij}(x)$ have an attractive physical interpretation as the probability of finding a parton of type i in a parton of type j with a fraction x of the longitudinal momentum of the parent parton and a transverse momentum squared much less than t.

* The interpretation as probabilities implies that the splitting function are positive definite for $x < 1$, and satisfy the sum rules

$$\int_0^1 dx \; P_{qq}(x) = 0$$

$$\int_0^1 dx \; x\left[P_{qq}(x) + P_{gq}(x)\right] = 0$$

$$\int_0^1 dx \; x\left[2n_f P_{fg}(x) + P_{gg}(x)\right] = 0$$

which correspond to quark number conservation and momentum conservation in the splittings of quarks and gluons, respectively.

Solution by moments

- Given $D_i(x,t)$ at some scale $t = t_0$, factorized structure of DGLAP equation means we can compute its form at any other scale.

- One strategy for doing this is to take moments (Mellin transforms) with respect to x:

$$\tilde{D}_i(N,t) = \int_0^1 dx\; x^{N-1}\; D_i(x,t)\;.$$

  Inverse Mellin transform is

$$D_i(x,t) = \frac{1}{2\pi i}\int_C dN\; x^{-N}\; \tilde{D}_i(N,t)\;,$$

  where contour C is parallel to imaginary axis to right of all singularities of integrand.

- After Mellin transformation, convolution in DGLAP equation becomes simply a product:

$$t\frac{\partial}{\partial t}\tilde{D}_i(x,t) = \sum_j \gamma_{ij}(N,\alpha_s)\tilde{D}_j(N,t)$$

where anomalous dimensions γ_{ij} are given by moments of splitting functions:

$$\gamma_{ij}(N,\alpha_s) = \sum_{n=0}^{\infty} \gamma_{ij}^{(n)}(N) \left(\frac{\alpha_s}{2\pi}\right)^{n+1}$$

$$\gamma_{ij}^{(0)}(N) = \tilde{P}_{ij}(N) = \int_0^1 dz\; z^{N-1}\; P_{ij}(z)$$

- From above expressions for $P_{ij}(z)$ we find

$$\gamma_{qq}^{(0)}(N) = C_F\left[-\frac{1}{2} + \frac{1}{N(N+1)} - 2\sum_{k=2}^{N}\frac{1}{k}\right]$$

$$\gamma_{qg}^{(0)}(N) = T_R\left[\frac{(2+N+N^2)}{N(N+1)(N+2)}\right]$$

$$\gamma_{gq}^{(0)}(N) = C_F\left[\frac{(2+N+N^2)}{N(N^2-1)}\right]$$

$$\gamma_{gg}^{(0)}(N) = 2C_A\left[-\frac{1}{12} + \frac{1}{N(N-1)} + \frac{1}{(N+1)(N+2)} - \sum_{k=2}^{N}\frac{1}{k}\right] - \frac{2}{3}N_f T_R\,.$$

- Consider combination of parton distributions which is flavour non-singlet, e.g. $D_V = D_{q_i} - D_{\bar{q}_i}$ or $D_{q_i} - D_{q_j}$. Then mixing with the flavour-singlet gluons drops out and solution for fixed α_s is

$$\tilde{D}_V(N,t) = \tilde{D}_V(N,t_0)\left(\frac{t}{t_0}\right)^{\gamma_{qq}(N,\alpha_s)}$$

- We see that dimensionless function D_V, instead of being scale-independent function of x as expected from dimensional analysis, has scaling violation: its moments vary like powers of scale t (hence the name anomalous dimensions).

- For running coupling $\alpha_s(t)$, scaling violation is power-behaved in $\ln t$ rather than t. Using leading-order formula $\alpha_s(t) = 1/b\ln(t/\Lambda^2)$, we find

$$\tilde{D}_V(N,t) = \tilde{D}_V(N,t_0)\left(\frac{\alpha_s(t_0)}{\alpha_s(t)}\right)^{d_{qq}(N)}$$

  where $d_{qq}(N) = \gamma_{qq}^{(0)}(N)/2\pi b$.

- Flavour-singlet distribution and quantitative predictions will be discussed later.

Scaling violation

- Bjorken scaling is not exact. Structure functions decrease at large x and grow at small x with increasing Q^2. This is due to Q^2 dependence of parton distributions, considered earlier. In present notation, they satisfy DGLAP evolution equations of form

$$t\frac{\partial}{\partial t}q(x,t) = \frac{\alpha_s(t)}{2\pi}\int_x^1 \frac{dz}{z}P(z)q\left(\frac{x}{z},t\right) \equiv \frac{\alpha_s(t)}{2\pi}P\otimes q$$

  where P is $q \to qg$ splitting function.

- Taking into account other types of parton branching that can occur in addition to $q \to qg$, we obtain coupled evolution equations

$$\begin{aligned}
t\frac{\partial q_i}{\partial t} &= \frac{\alpha_s(t)}{2\pi}\left[P_{qq}\otimes q_i + P_{qg}\otimes g\right] \\
t\frac{\partial \bar{q}_i}{\partial t} &= \frac{\alpha_s(t)}{2\pi}\left[P_{qq}\otimes \bar{q}_i + P_{qg}\otimes g\right] \\
t\frac{\partial g}{\partial t} &= \frac{\alpha_s(t)}{2\pi}\left[P_{gq}\otimes \sum(q_i+\bar{q}_i) + P_{gg}\otimes g\right] \ .
\end{aligned}$$

- Lowest-order splitting functions derived earlier. More generally they are power series in α_s, same for deep inelastic scattering (spacelike branching) and jet fragmentation (timelike branching) in leading order, but differing in higher orders. Consequently, behaviour of structure functions at small x is different from that of jet fragmentation functions.

- For the present, concentrate on larger x values ($x \gtrsim 0.01$), where PT expansion converges better.

- Recall solution of evolution equations for flavour non-singlet combinations V, e.g. $q_i - \bar{q}_i$ or $q_i - q_j$. Mixing with gluons drops out and

$$t\frac{\partial}{\partial t}V(x,t) = \frac{\alpha_s(t)}{2\pi}P_{qq} \otimes V \ .$$

Taking moments (Mellin transform)

$$\tilde{V}(N,t) = \int_0^1 dx\; x^{N-1}\; V(x,t)$$

we find

$$t\frac{\partial}{\partial t}\tilde{V}(N,t) = \frac{\alpha_s(t)}{2\pi}\gamma_{qq}^{(0)}(N)\;\tilde{V}(N,t)$$

where $\gamma_{qq}^{(0)}(N)$ is Mellin transform of $P_{qq}^{(0)}$. Solution is

$$\tilde{V}(N,t) = \tilde{V}(N,0)\left(\frac{\alpha_s(0)}{\alpha_s(t)}\right)^{d_{qq}(N)}$$

where $d_{qq}(N) = \gamma_{qq}^{(0)}(N)/2\pi b$.

- Now $d_{qq}(1) = 0$ and $d_{qq}(N) < 0$ for $N \geq 2$. Thus as t increases $\tilde{V}(N,t)$ is constant for $N = 1$ and *decreases* and at larger N.

- Since larger-N moments emphasize larger x, this means that $D_V(x,t)$ *decreases* at large x and increases at small x. (Physically, this is due to increase in the phase space for gluon emission by quarks as t increases, leading to loss of momentum.) This is clearly visible in data.

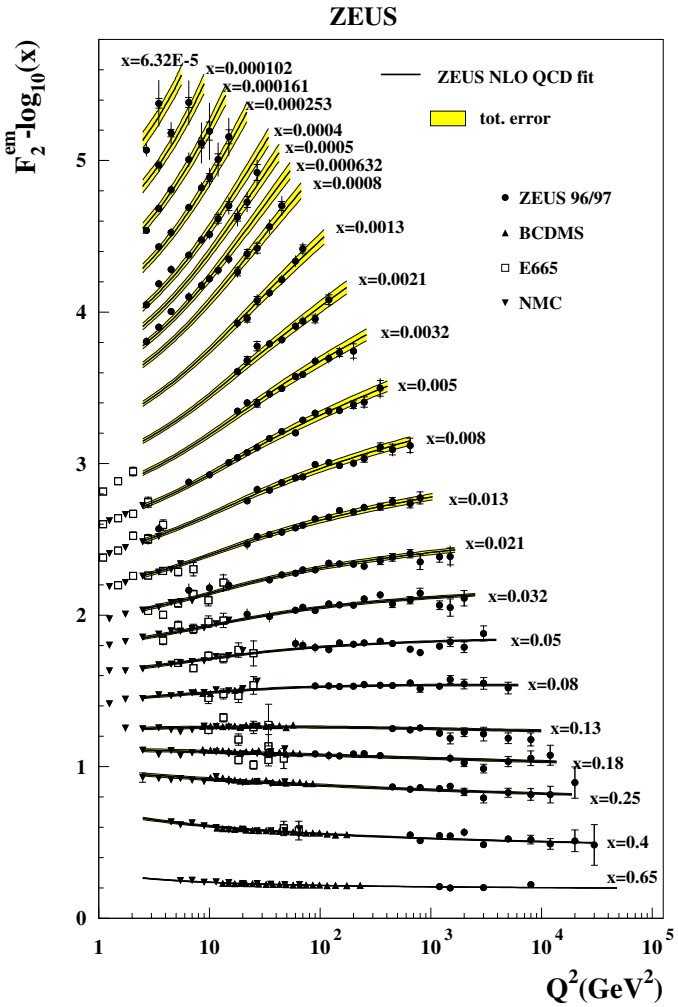

- For flavour-singlet combination, define

$$\Sigma = \sum_i \left(q_i + \bar{q}_i\right) .$$

Then we obtain

$$\begin{aligned} t\frac{\partial \Sigma}{\partial t} &= \frac{\alpha_s(t)}{2\pi}\left[P_{qq} \otimes \Sigma + 2N_f P_{qg} \otimes g\right] \\ t\frac{\partial g}{\partial t} &= \frac{\alpha_s(t)}{2\pi}\left[P_{gq} \otimes \Sigma + P_{gg} \otimes g\right] . \end{aligned}$$

- Thus flavour-singlet quark distribution Σ mixes with gluon distribution g: evolution equation for moments has matrix form

$$t\frac{\partial}{\partial t}\begin{pmatrix} \tilde{\Sigma} \\ \tilde{g} \end{pmatrix} = \begin{pmatrix} \gamma_{qq} & 2N_f\gamma_{qg} \\ \gamma_{gq} & \gamma_{gg} \end{pmatrix}\begin{pmatrix} \tilde{\Sigma} \\ \tilde{g} \end{pmatrix}$$

- Singlet anomalous dimension matrix has two real eigenvalues $\gamma_\pm$ given by

$$\gamma_\pm = \tfrac{1}{2}[\gamma_{gg} + \gamma_{qq} \pm \sqrt{(\gamma_{gg} - \gamma_{qq})^2 + 8N_f\gamma_{gq}\gamma_{qg}}] \; .$$

- Expressing $\tilde{\Sigma}$ and $\tilde{g}$ as linear combinations of eigenvectors $\tilde{\Sigma}_+$ and $\tilde{\Sigma}_-$, we find they evolve as superpositions of terms of above form with $\gamma_\pm$ in place of γ_{qq}.

Small x

- At small x, corresponding to $N \to 1$, $\gamma_+ \to \gamma_{gg} \to \infty$, $\gamma_- \to \gamma_{qq} \to 0$. Therefore structure functions grow rapidly at small x.

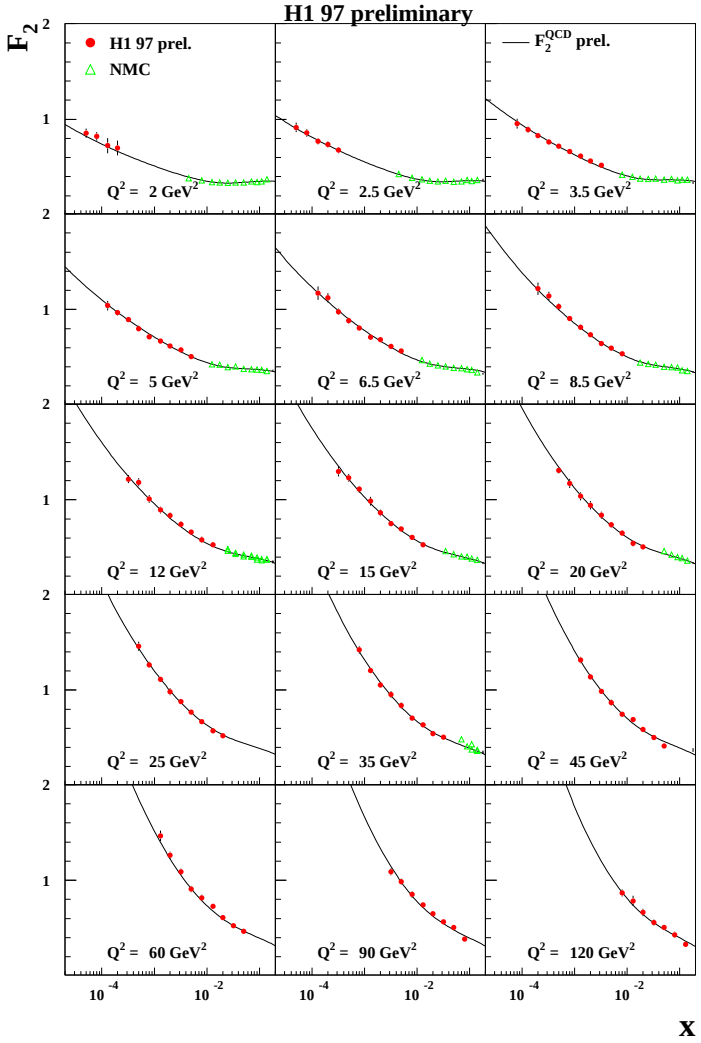

- Kinematic region at HERA is shown in figure.

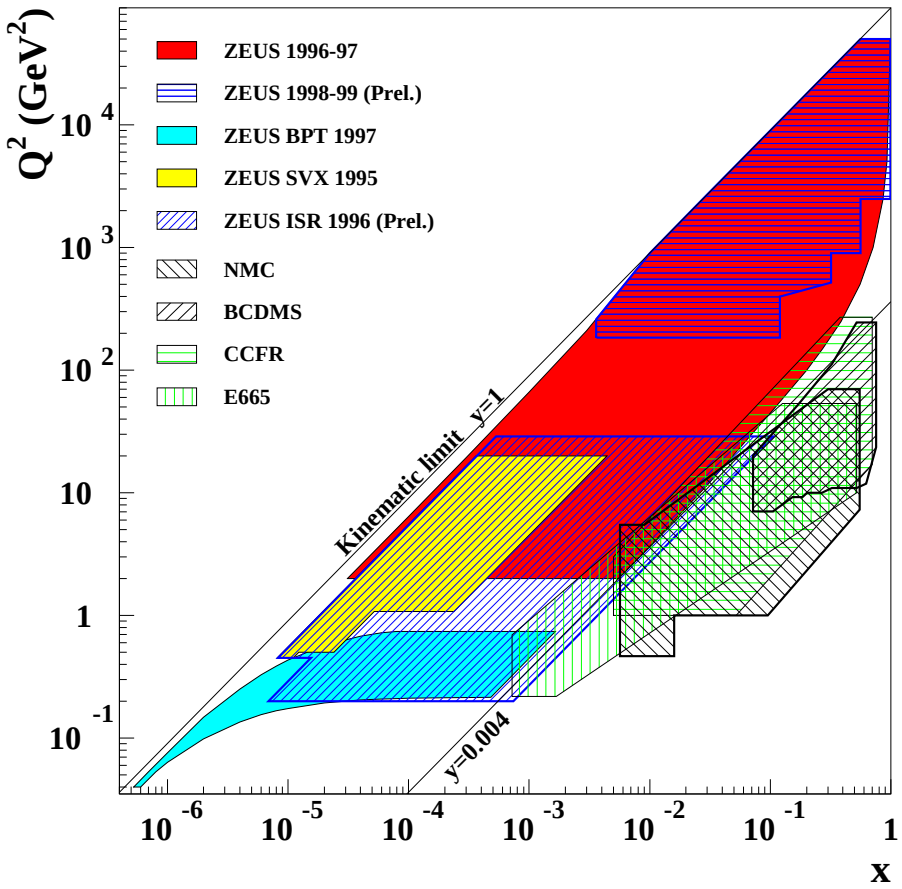

⋆ Note that values of Q^2 and x are correlated at HERA.

Hadron-hadron processes

- In hard hadron-hadron scattering, constituent partons from each incoming hadron interact at short distance (large momentum transfer Q^2).

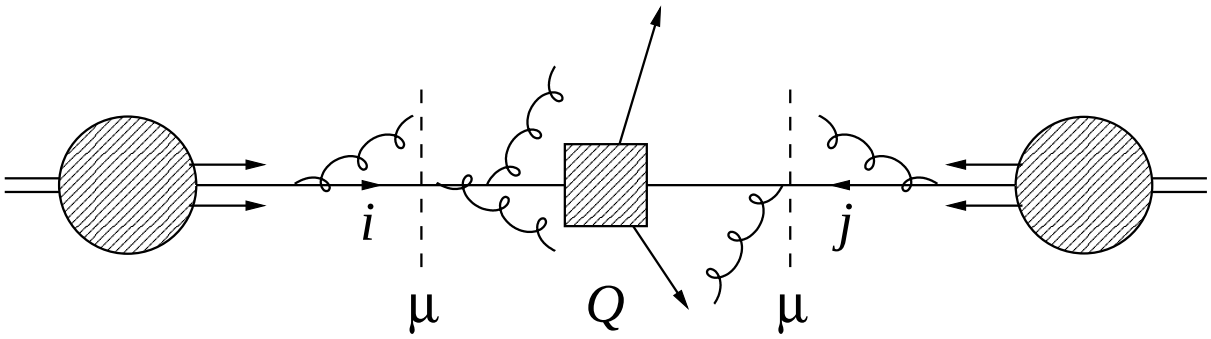

- For hadron momenta P_1, P_2 ($S = 2P_1 \cdot P_2$), form of cross section is

$$\begin{aligned}\sigma(S) &= \sum_{i,j} \int dx_1 dx_2 D_i(x_1, \mu^2) D_j(x_2, \mu^2) \\ &\quad \times \hat{\sigma}_{ij}(\hat{s} = x_1 x_2 S, \alpha_s(\mu^2), Q^2/\mu^2)\end{aligned}$$

where μ^2 is factorization scale and $\hat{\sigma}_{ij}$ is subprocess cross section for parton types i, j.

- ⋆ Notice that factorization scale is in principle arbitrary: affects only what we call part of subprocess or part of initial-state evolution (parton shower).
- ⋆ Unlike e^+e^- or ep, we may have interaction between spectator partons, leading to *soft underlying event* and/or *multiple hard scattering*.

Jet production

- Lowest-order subprocess for purely hadronic jet production is $2 \to 2$ scattering $p_1 + p_2 \to p_3 + p_4$

$$\frac{E_3 E_4 d^6\hat{\sigma}}{d^3\boldsymbol{p}_3 d^3\boldsymbol{p}_4} = \frac{1}{32\pi^2\hat{s}}\overline{\sum}|\mathcal{M}|^2\,\delta^4(p_1 + p_2 - p_3 - p_4)\ .$$

- Many processes even at $\mathcal{O}(\alpha_s^2)$:

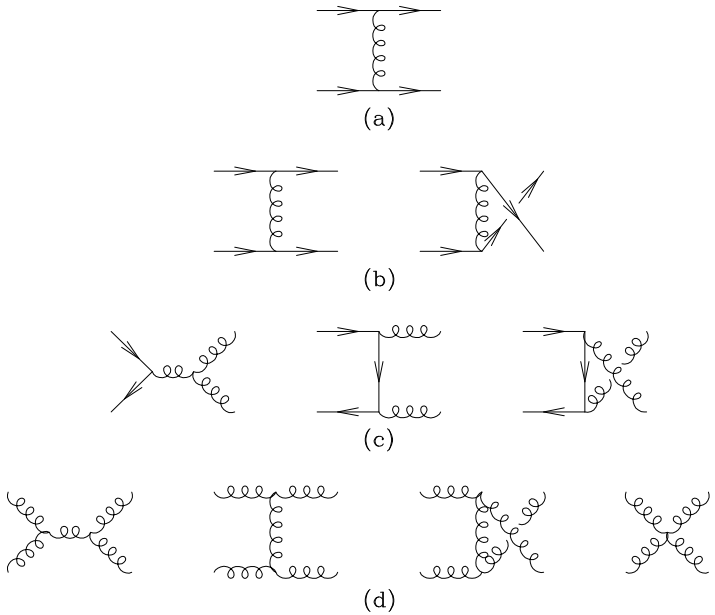

- Single-jet inclusive cross section obtained by integrating over one outgoing momentum:

$$\frac{E d^3\hat{\sigma}}{d^3\boldsymbol{p}} = \frac{d^3\hat{\sigma}}{d^2\boldsymbol{p}_T dy} \longrightarrow \frac{1}{2\pi E_T}\frac{d^3\hat{\sigma}}{dE_T\, d\eta} = \frac{1}{16\pi^2\hat{s}}\overline{\sum}|\mathcal{M}|^2\,\delta(\hat{s}+\hat{t}+\hat{u})$$

where (neglecting jet mass)

$$E_T \equiv E\sin\theta = |\boldsymbol{p}_T|\,, \quad \eta \equiv -\ln\tan(\theta/2) \;=\; y\,.$$

- Jets in hadron-hadron usually defined using cone algorithm: combine all hadrons h with

$$\Delta R_{hJ} \equiv \sqrt{(\eta_h-\eta_J)^2+(\phi_h-\phi_J)^2} < R$$

where η_J, ϕ_J refer to jet axis, chosen to maximize jet E_T, and $R \sim 0.7$ is cone size.

- Use η rather than θ for invariance under longitudinal boosts: $x_1 \to a x_1$, $x_2 \to x_2/a$ gives

$$\eta_{h,J} \to \eta_{h,J} + \ln a$$

so $\eta_h - \eta_J$ is invariant.

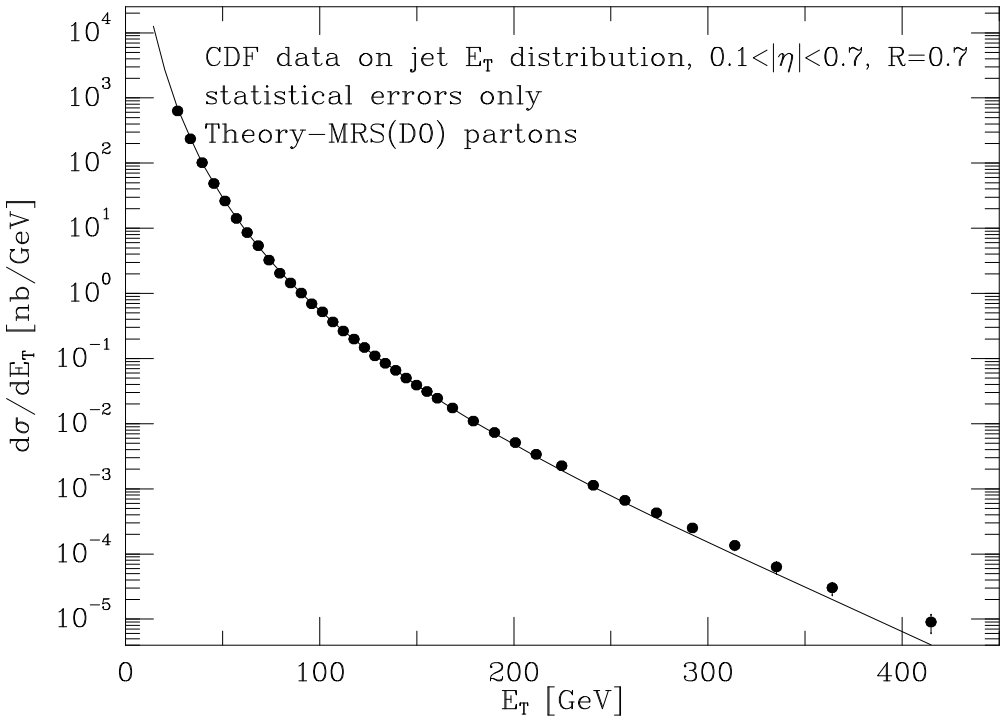

- Slight excess at large E_T caused excitement, but can be reduced/removed by adjusting gluon distribution.

- Contribution of different parton combinations ij determined by subprocess cross sections and parton distributions.

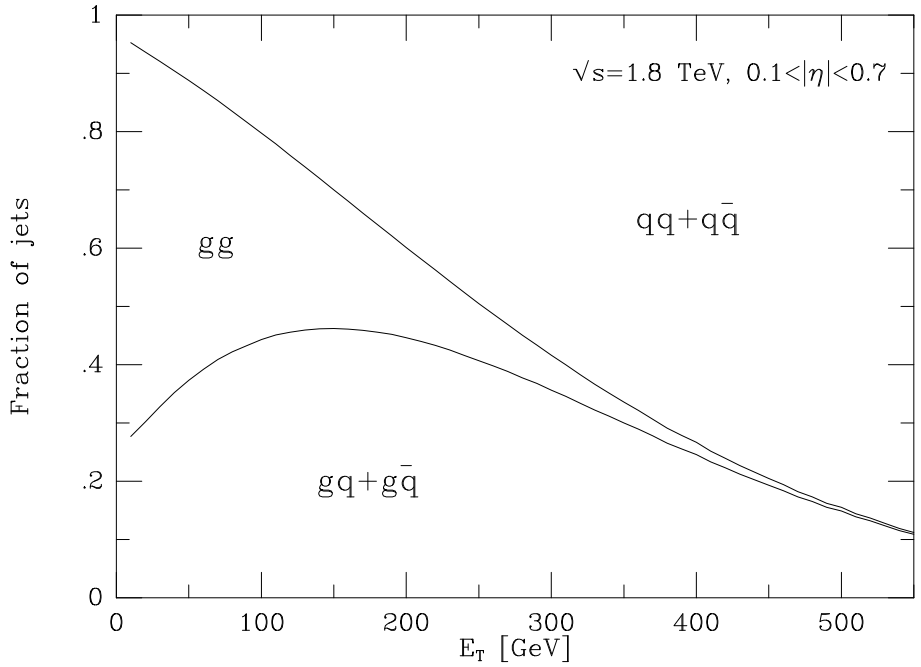

- Quarks dominate at large E_T since this selects large $x_{1,2}$:

$$\hat{s} = x_1 x_2 S > 4E_T^2$$

Lattice QCD

* At large distances the strong coupling becomes large and perturbation theory is useless. It is hence important to have a nonperturbative formulation of QCD. The most developed method for this is lattice QCD.

* In lattice QCD one defines a Euclidean version of QCD on a discrete (hypercubic) four-dimensional space-time lattice consisting of hypercubes with sides of length a. By this UV divergences are regularized since it implies a cut-off of order $\frac{\pi}{a}$ on all momenta.

* Lattice discretization breaks Lorentz invariance but can be done in such a way that local gauge invariance is preserved.

* Ultimately, one is interested in the continuum limit of small lattice spacing a.

* The lattice formulation of QCD makes contact with statistical mechanics and allows one to use its methods for direct numerical computations.

* First continue from Minkowski space to Euclidean space by performing Wick rotation $x^4 = ix^0$, $\partial^4 = -i\partial^0$. This leads to a real, positive action for gauge fields, and hence allows one easily to identify most important field configurations which give smallest action.

* Recall colour string operator

$$S(y,x) = \mathcal{P} \exp\left[-ig \int_x^y dz_\mu \, t \cdot A^\mu(z)\right]$$

$$= 1 - ig \int_x^y dz_\mu \, t \cdot A^\mu(z) - g^2 \int_z^y dz_\mu \, t \cdot A^\mu(z) \int_x^z dw_\mu \, t \cdot A^\mu(w) + \ldots$$

Under gauge transformation Ω it transforms as

$$S(y,x) \longrightarrow \Omega(y) \, S(y,x) \, \Omega^{-1}(x).$$

Hence the product of string operators along a closed path is gauge invariant.

* Lattice QCD uses link variable $\mathcal{U}$ which is discretized version of string operator S as fundamental quantity to represent gauge fields. Link variables are

$$\mathcal{U}_\mu(x) = S(x, x+\mu a)$$

with μ the unit vector along link direction:

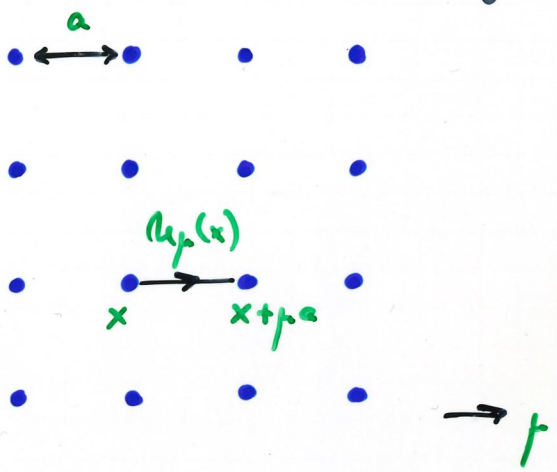

* Action for gauge field is determined by product of link variables around a square path of side length a, called a plaquette,

$$\mathcal{U}_\square = \mathcal{U}_\mu(x)\,\mathcal{U}_\nu(x+a\mu)\,\mathcal{U}_{-\mu}(x+a\mu+a\nu)\,\mathcal{U}_{-\nu}(x+a\nu)$$
$$= \mathcal{U}_\mu(x)\,\mathcal{U}_\nu(x+a\mu)\,\mathcal{U}_\mu^+(x+a\nu)\,\mathcal{U}_\nu^+(x)$$

Total action for $SU(3)$ pure gauge theory is sum over plaquettes,

$$S_G = \beta \sum_\square \left[1 - \tfrac{1}{3}\,\mathrm{Re}\,\mathrm{Tr}\,\mathcal{U}_\square(x)\right]$$

with β a constant related to the gauge coupling.

* This action can be shown to reproduce pure QCD action in the continuum limit.

* Physical predictions are made by evaluating the integral over all configurations of the fields, weighted by the action. Practically, the most frequently used method for this is direct Monte Carlo evaluation.

* Quarks can be implemented as well (with some technical difficulties though), and reside on the lattice sites. Practically, the simulation of dynamical quarks on the lattice is very costly in computer time. As a result, many calculations use the quenched approximation in which dynamical quarks are left out. The quenched approximation is only (!) motivated by saving in computer time. Its validity can be tested only a posteriori.

* In quenched approximation the expectation value of any operator $O(U)$ is

$$\langle O \rangle = \frac{\int \{dU_\mu\}\, O(U) \exp[-S_G(U)]}{\int \{dU_\mu\} \exp[-S_G(U)]}$$

to be evaluated numerically. Here the functional integrals are approximated by integrating over all the links (and quark fields in case of an unquenched calculation) at all the points of the lattice.

* In practice, lattice must be large enough and the lattice spacing must be small enough for a given observable.

* An example for a lattice result is the quark - antiquark potential shown earlier.